Enhancement of Free-Radical Chain Rearrangement, Cyclization, and Hydrogenolysis during Thermolysis of Surface-Immobilized Bibenzyl: Implications for Coal Chemistry[1,2]

A. C. Buchanan, III,* T. Don J. Dunstan, Emily C. Douglas, and Marvin L. Poutsma*

Contribution from the Chemistry Division, Oak Ridge National Laboratory, Oak Ridge, Tennessee 37831. *Received March 18, 1986*

Abstract: Condensation of p-$HOC_6H_4CH_2CH_2C_6H_5$ (**15c**) with the surface hydroxyls of fumed silica gave a surface-immobilized form of bibenzyl (**16c**) whose thermolysis was compared with that studied earlier for liquid and gaseous bibenzyl (**1**). The objective was to explore the effects of restricted mobility on a multipathway free-radical reaction, with particular emphasis on modeling dimethylene linking units between aromatic clusters in coal. The initial rate of thermolysis of **16c** at 350–400 °C was accelerated some fourfold compared with **1**, and the product composition was notably altered. The major initial product classes, in order of decreasing amounts, were the following: (1) rearrangement to form surface-attached 1,1-diphenylethane (**18**); (2) cyclization–dehydrogenation to form surface-attached 9,10-dihydrophenanthrene (**20**) (and subsequently surface-attached phenanthrene (**21**)); (3) symmetrical cleavage to form both surface-attached and gas-phase toluene (**19** and **3**) in similar amounts; (4) dehydrogenation to form surface-attached stilbene (**24**); and (5) unsymmetrical hydrogenolysis to form surface-attached ethylbenzene (**22**) plus gas-phase benzene (**10**) and the analogous pair, **23** plus **11**, in similar amounts. For liquid **1**, cyclization and unsymmetrical cleavage had been barely detectable and rearrangement was only a minor pathway. The rate constant for unimolecular C–C homolysis in **16c**, based on **3** and **19**, was $10^{15.3}\exp(-62\,900/RT)$ s^{-1}, not significantly different from that of **1** and not dependent on surface coverage. However, the initial extent of rearrangement, expressed as a chain length, was accelerated some 30-fold compared with that of liquid **1**; cyclization and unsymmetrical cleavage were similarly enhanced. These accelerations, in contrast to C–C homolysis, decreased both with decreasing initial surface coverage (0.465–0.104 mmol g^{-1}; 1.55–0.32 bibenzyl moieties nm^{-2}) and increasing conversion level. These three processes are all inherently chain reactions cycling through $PhCH_2\dot{C}HPh$ (**4**) or its surface-attached analogue **35**. The observed increases in chain length accompanying surface immobilization are attributed to serious restrictions on bimolecular radical–radical termination events while hydrogen atom transfers between surface-attached radicals, such as benzyl (**34**) and 2,2-diphenylethyl (**36**), and adjacent **16c** species remain possible, although coverage-dependent. This conclusion is reinforced by the virtual absence among the products of surface-attached analogues of 1,2,3,4-tetraphenylbutane, the expected major product if **35** were free to diffuse. Alternate mechanisms for cyclization are subjected to thermochemical kinetic analysis; a pathway beginning with intramolecular 1,4-hydrogen transfer in **4** (or **35**) appears more likely than one beginning with direct intramolecular cyclization. It is suggested that cyclization–dehydrogenation and unsymmetrical hydrogenolysis are mechanistically coupled through the intermediacy of hydrogen atoms. Implications for coal conversion of the effects of restricted radical mobility during thermal decomposition of cross-linked polymers are noted.

Thermal decompositions of selected aralkyl hydrocarbons and ethers have been studied recently by several groups because these compounds serve as models for structural units in coal. Coal has a covalently cross-linked, macromolecular structure which causes it to be insoluble and nonvolatile.[3-5a] Most practiced and envisioned processes for conversion of coal[5b-g,6-8] to commercially useful products, ranging from metallurgical coke to "synthetic" petroleum replacements to petrochemical feedstocks, involve thermally induced cleavage of bonds to break up this cross-linked framework. Bond breaking occurs at significant rates near 400 °C and generates free radicals[9] by bond homolysis or β-scission processes. In the presence of hydrogen atom donors, the radical centers may be converted to stable end groups. Given the breaking of enough bonds, the final products will be gases and soluble liquids of modest molecular weight. In the absence of hydrogen atom donors, the radicals may instead undergo "condensation" reactions which lead to solid residues even more cross-linked and refractory than the starting coal. Attempts to understand the thermal chemistry of coal at the molecular level are severely hampered by its combination of inherent properties: a wide variety of structural units (aromatic, hydroaromatic, and heterocyclic aromatic clusters joined by short aliphatic and ether linkages) and functional groups (phenolic hydroxyls, basic nitrogens, carboxyls) in a cross-linked macromolecular array with no regularity or repeating units.[3-5a] One simplifying experimental approach is the study of individual model compounds which highlight selected structural features in coal.

Interpretive extrapolations from model compound behavior to coal must be made with cognizance of many complicating features inherent to coal. Examples are the need to consider properly structure–reactivity correlations, interactions among functional groups, and catalysis by coal minerals. The particular complication which stimulated the present study is possible modifications of

(1) Research supported by the Division of Chemical Sciences, Office of Basic Energy Sciences, U.S. Department of Energy under Contract DE-AC05-840R21400 with Martin Marietta Energy Systems. The U.S. D.O.E. Postgraduate Research Training Program appointment held by T.D.J.D. was administered by the Oak Ridge Associated Universities.

(2) Paper 5 in the series: "Thermolysis of Model Compounds for Coal"; for paper 4 and preliminary communication on present work, see: Poutsma, M. L.; Douglas, E. C.; Leach, J. E. *J. Am. Chem. Soc.* **1984**, *106*, 1136.

(3) Green, T.; Kovac, J.; Brenner, D.; Larsen, J. W. In *Coal Structure*; Meyers, R. A., Ed.; Academic Press: New York, 1982; Chapter 6.

(4) Davidson, R. M. In *Coal Science*; Gorbarty, M. L., Larsen, J. W., Wender, I., Eds.; Academic Press: New York, 1982; Vol. 1.

(5) Elliott, M. A., Ed. *Chemistry of Coal Utilization*; Wiley-Interscience: New York, 1981; Suppl. Vol. 2: (a) Wender, I.; Heredy, L. A.; Neuworth, M. B.; Dryden, I. G. C. Chapter 8; (b) Howard, J. B. Chapter 12; (c) Gorin, E. Chapter 27; (d) Alpert, S. B.; Wolk, R. H. Chapter 28; (e) Eisenhut, W. Chapter 14; (f) Aristoff, E.; Rieve, R. W.; Shalit, H. Chapter 16; (g) McNeil, D. Chapter 17.

(6) Whitehurst, D. D.; Mitchell, T. O.; Farcasiu, M. *Coal Liquefaction*; Academic Press: New York, 1980.

(7) Gavalas, G. R. *Coal Pyrolysis*; Elsevier: Amsterdam, 1982.

(8) Berkowitz, N. *An Introduction to Coal Technology*; Academic Press: New York, 1980.

(9) Curran, G. P.; Struck, R. T.; Gorin, E. *Ind. Eng. Chem., Proc. Des. Dev.* **1967**, *6*, 166. Wiser, W. H. *Fuel* **1968**, *47*, 475. Neavel, R. C. *Ibid.* **1976**, *55*, 237.

0002-7863/86/1508-7703$01.50/0

Table I. Product Distributions (mol %) from Thermolysis of Bibenzyl (**1**) at 400 °C

time (min)	15[a]	15[a]	15[b]	60[b]
phase	gas (54 kPa)[c]	liquid[d]	liquid[d]	liquid[d]
conversion (%)	1.7[e]	1.4[e]		7.5
product:				
$PhCH_3$ (**3**)	53.0	56.1	56	58
$(PhCH_2CHPh-)_2$ (**7**)	17.5	20.9	23	8
$(PhCH_2)_2CHPh$ (**5**)	17.7	2.1	2	1.5
PhCH=CHPh (**6**)	9.6	9.9	9	17
Ph_2CHCH_3 (**9**)	1.1	10.5	10	10
PhH (**10**)	1.2	0.6		0.9
$PhCH_2CH_3$ (**11**)				1.0
Ph_2CH_2 (**12**)				0.8
phenanthrene (**13**)				0.9
H_2				1.7
CH_4				0.08

[a] Reference 12. [b] Reference 13; values visually estimated from published figures. [c] Concentration of **1** is 9.7×10^{-3} M. [d] Concentration of **1** is 4.0 M (ref 13). [e] Even at these very low conversions, there is a modest distortion from initial behavior because of the high thermal lability of **7** with respect to secondary formation of **1** plus **6**.[12,13]

free-radical behavior resulting from restricted translational mobility.

Model compound studies are typically performed in the gaseous or liquid state. Radicals formed by bond homolysis are free to diffuse independently and typically move some distance apart before reacting further. In contrast, radical centers formed by breaking one bond in a cross-linked macromolecular structure such as coal still remain bonded to the residual framework. Hence, their mobility with respect to each other and the rest of the coal structure would be expected to be significantly restricted. We chose to explore the consequences of restricted mobility on radical reactivity by studying the thermolysis of model compounds which had been immobilized by covalent attachment to an inert solid.[10] Studies of the thermolysis and/or photolysis of radical precursors physically adsorbed on solids[11] are being pursued by several groups. However, we are not aware of thermolysis studies involving covalent attachment to surfaces by bonds robust enough to survive the relatively high temperatures (400 °C) required for our purposes.

Thermolysis of Bibenzyl. It was desirable to begin an exploration of surface immobilization with a model compound for coal whose fluid-state behavior was already well-understood. No example has received as much attention as 1,2-diphenylethane (bibenzyl; **1**) which represents dimethylene connecting links between aromatic clusters in coal. The fluid-state thermolyses of **1** can be understood in terms of steps 1–6.

A typical product distribution from thermolysis of **1** as a dilute *gas* (54 kPa = 0.5 atm) at 400 °C after only 1.7% conversion[12] is shown in column 2 of Table I. Only steps 1–4 are necessary to account for the four major products: toluene (**3**), 1,2,3,4-tetraphenylbutane (**7**), 1,2,3-triphenylpropane (**5**), and stilbene (**6**). Symmetrical homolysis of **1** produces benzyl radicals (**2**), most of which decay by hydrogen atom transfer from **1** to form **3** and the 1,2-diphenylethyl radical (**4**). Radical **4** is consumed by radical–radical interactions with **2** or with itself. In each case, coupling (to form **5** or **7**) predominates over disproportionation (to form **3** or **1** and **6**). Increasing pressure of **1** increases the **7**:**5** ratio[12] as more of **2** is captured in step 2 at the expense of step 3.

Note that **1** is consumed by two distinct pathways: homolysis in step 1 and induced decomposition by hydrogen atom transfer

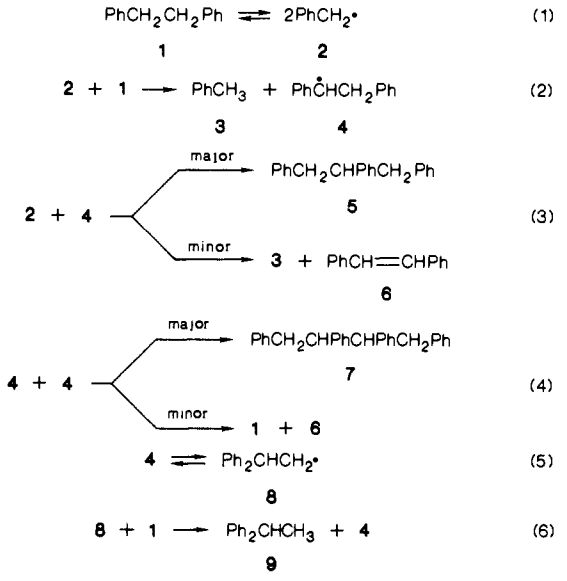

in step 2. To isolate the homolysis process and thereby measure k_1, a "tetralin carrier" technique[14] can be used in which this good hydrogen atom donor is added to consume **2** and thereby to protect **1** from the induced decomposition pathway. Mutually consistent gas-phase tetralin-carrier studies by Stein and co-workers[15] and Sato and co-workers[16] over temperature ranges centered near 415 °C give an average value of $k_1 = 10^{15.05} \exp(-61\,400/RT)$ s^{-1}. This kinetic parameter, $E_{1,688}$, coupled with group additivity estimates[18] of $\overline{\Delta C_p}°_1$, suggests a bond dissociation enthalpy[17] of $\Delta H°_{298,1} \simeq 61.8$ kcal mol^{-1} (see Appendix 1 for details). Heat of formation data for **1**[19] and **2**[17] suggest a value of 61.4 kcal mol^{-1}. The kinetic parameter $A_{1,688}$, coupled with an estimate[20] of $A_{-1} = k_{-1} \simeq 10^{9.85}$ M^{-1} s^{-1}, suggests a bond dissociation entropy of $\Delta S°_{298,1} \simeq 33.1$ cal mol^{-1} K^{-1} (pressure standard state). Group additivity estimates[18] for the entropies of **1** and **2** suggest a value of 33.4 cal mol^{-1} K^{-1}. Thus, within the uncertainties of these estimation procedures, the agreement between existing thermochemical and kinetic data for homolysis of **1** is clearly excellent.[21]

Based on simplification according to the "geomerical mean rule"[22] ($k_t \equiv k_{-1} \simeq k_4 \simeq k_3/2$), steady-state analysis of steps 1–4 gives an expression (see Appendix 1) for the ratio of coupling products:

$$(7)/(5) \simeq k_2(1)^{1/2}/4(k_1k_t)^{1/2}$$

Inserting k_1,[15,16] k_t (see above), and the experimental (**7**)/(**5**) data gives an estimate of $k_{673,2} \simeq 1.2 \times 10^4$ M^{-1} s^{-1}. If $A_2 \simeq 10^{8.0}$ M^{-1} s^{-1} (per H), as is typically observed for hydrogen atom transfers between carbon centers,[13,23] this estimate of $k_{673,2}$ leads

(10) A complementary approach involving thermolysis of polymeric models for coal is in progress by others: Squire, K. R.; Solomon, P. R.; DiTaranto, M. B.; Carangelo, R. M. *Prepr., Div. Fuel Chem., Am. Chem. Soc.* **1985**, *30* (1), 386. Squires, T. G.; Smith, B. F.; Winnans, R. E.; Scott, R. G.; Hayatsu, R. *Proc. 1983 Int. Conf. Coal Sci., Pittsburgh*, **1984**, 292.

(11) (a) Frederick, B.; Johnston, L. J.; DeMayo, P.; Wong, S. K. *Can. J. Chem.* **1984**, *62*, 403. Leffler, J. E.; Barbas, J. T. *J. Am. Chem. Soc.* **1981**, *103*, 7768. Baretz, B. H.; Turro, N. J. *Ibid.* **1983**, *105*, 1309. (b) Turro, N. J.; Wan, P. *Ibid.* **1985**, *107*, 678.

(12) Poutsma, M. L. *Fuel* **1980**, *59*, 335.

(13) Miller, R. E.; Stein, S. E. *J. Phys. Chem.* **1981**, *85*, 580.

(14) Rüchardt, C.; Beckhaus, H.-D. *Angew. Chem., Int. Ed. Engl.* **1980**, *19*, 424.

(15) Stein, S. E.; Robaugh, D. A.; Alfieri, A. D.; Miller, R. E. *J. Am. Chem. Soc.* **1982**, *104*, 6567.

(16) Sato, Y.; Yamakawa, T.; Onishi, R.; Kameyama, H.; Amano, A. *J. Jpn. Petrol. Inst.* **1978**, *21*, 110.

(17) McMillen, D. F.; Golden, D. M. *Annu. Rev. Phys. Chem.* **1982**, *33*, 493.

(18) Benson, S. W. *Thermochemical Kinetics*; Wiley-Interscience: New York, 1976.

(19) (a) Coleman, D. J.; Pilcher, G. *Trans. Faraday Soc.* **1966**, *62*, 821. (b) Osborn, A. G.; Scott, D. W. *J. Chem. Thermodyn.* **1980**, *12*, 429. Morawetz, E. *Ibid.* **1972**, *4*, 455.

(20) Rossi, M.; King, K. D.; Golden, D. M. *J. Am. Chem. Soc.* **1979**, *101*, 1223. Van den Bergh, H. E.; Callear, A. B. *Trans. Faraday Soc.* **1970**, *66*, 2681.

(21) A recent theoretical gas-phase value of $k_1 = 10^{10.2} \exp(-45\,300/RT)$ s^{-1} [Petrocelli, F. P.; Klein, M. T. *Macromolecules* **1984**, *17*, 161] must thus be suspect on thermochemical kinetic grounds.

(22) Paul, H.; Segaud, C. *Int. J. Chem. Kinet.* **1980**, *12*, 637. Kerr, J. A. In "*Free Radical*"; Kochi, J. K., Ed.; Wiley: New York, 1973; Vol. 1, Chapter 1.

(23) Poutsma, M. L.; Dyer, C. W. *J. Org. Chem.* **1982**, *47*, 4903.

to $E_2 \simeq 13.9$ kcal mol^{-1}. This is fully consistent with a separate thermochemical kinetic estimate[23] of $E_2 \simeq 14.2$ kcal mol^{-1} which included no experimental data from thermolysis of **1**.[24]

A typical *liquid-phase* product distribution at 400 °C and ~1.5% conversion[12,13] is shown in columns 3 and 4 of Table I. Whereas **5** has almost disappeared, a new product, 1,1-diphenylethane (**9**), has gained stoichiometric significance. Skeletal rearrangement to form **9** proceeds through rearranged radical **8** and steps 5 and 6, which constitute a repeating chain. Hence, in the liquid phase, there are three competitive pathways which consume **1**: homolysis; induced decomposition to give the hydrogen-poor products **5**, **6**, and **7**; and rearrangement.

Two mutually consistent liquid-phase tetralin-carrier studies by Stein and co-workers[15] and by McMillen and co-workers[27] give $k_1 = 10^{16.5} \exp(-66\,600/RT)$ s^{-1}.[28] The slight depression in k_1 compared with the gas phase $[(k_{1,liq}/k_{1,gas})_{688} \simeq 0.6]$ and the largely compensating elevations in both A_1 and E_1 have been attributed[15] to a cage effect.

The expression developed above for the ratio (**7**)/(**5**) has a half-order dependence on (**1**) and thus predicts a 20-fold increase in this ratio between gas (54 kPa) and neat liquid $[(4/0.0097)^{1/2}]$, whereas the data in Table I show a 10-fold change. This small discrepancy may well be within the error limits of the approximations made involving k_t. In any case, the phase change does not produce any *large* changes in the elementary rate constants.

We define a chain length for rearrangement, L_{rearr}, as the ratio of the moles of rearranged product **9** formed in step 6 to the moles of chain-carrying radical 4 produced in step 2. Since step 2 is the only significant source of **3**, $L_{rearr} = (\mathbf{9})/(\mathbf{3}) \simeq 0.19$ for the neat liquid at 400 °C. In the steady-state approximation for the liquid phase where steps 3 and −1[24] are insignificant:

$$L_{rearr} \simeq \left(\frac{1}{2}\right)\left(\frac{1}{k_1 k_t}\right)^{1/2} \frac{k_5 k_6(\mathbf{1})^{1/2}}{\{k_{-5} + k_6(\mathbf{1})\}}$$

Recent data for a 30-fold variation in (**1**) in biphenyl as solvent have shown L_{rearr} to have a 0.50 ± 0.03 power dependence on (**1**).[31] The decrease in L_{rearr} in going to the gas phase indicates a similar dependence. Hence, we conclude that the expression can be simplified to:

$$L_{rearr} \simeq \left(\frac{1}{2}\right)\left(\frac{1}{k_1 k_t}\right)^{1/2} K_5 k_6(\mathbf{1})^{1/2}$$

which corresponds to $k_{-5} >> k_6(\mathbf{1})$.[32]

Product data at the somewhat higher conversion level of 7.5%[13] (column 5 of Table I) demonstrate the rapid secondary conversion of **7** to **6**. They also provide more reliable data concerning two trace processes:[12,13,21] unsymmetrical cleavage of **1** to form benzene (**10**) and ethylbenzene (**11**) and of cyclization–dehydrogenation to form phenanthrene (**13**) and hydrogen. Possible mechanisms for these very minor reactions have been discussed.[13,25] However, analytical restraints on measuring trace products at very low conversions have left some doubt whether **10**, **11**, and **13** are truly primary products or whether they result from secondary reactions.

Unsymmetrical hydrogenolysis to form **10** and **11** is promoted by high pressures of molecular hydrogen.[33] Vernon[33] proposed steps 7–9 to account for this added reaction pathway. Hydrogen serves as a hydrogen atom donor in step 7. Step 8 is an example

$$\underset{\mathbf{2}}{\mathrm{PhCH_2}\cdot} + \mathrm{H_2} \rightarrow \underset{\mathbf{3}}{\mathrm{PhCH_3}} + \mathrm{H}\cdot \qquad (7)$$

$$\mathrm{H}\cdot + \underset{\mathbf{1}}{\mathrm{PhCH_2CH_2Ph}} \rightarrow \underset{\mathbf{10}}{\mathrm{PhH}} + \underset{\mathbf{14}}{\mathrm{PhCH_2CH_2}\cdot} \qquad (8)$$

$$\mathbf{14} + \mathbf{1}\ (\mathrm{H_2}) \rightarrow \underset{\mathbf{11}}{\mathrm{PhCH_2CH_3}} + \underset{\mathbf{4}}{\mathrm{PhCHCH_2Ph}}\ (\mathrm{H}\cdot) \qquad (9)$$

of a well-known hydrodealkylation pathway which occurs by ipso attack of hydrogen atom on alkylaromatics to generate an intermediate cyclohexadienyl radical followed by reversal in the thermochemically more favorable direction to expel an alkyl radical, in this case **14**.[34]

Results

Procedures for Synthesis, Analysis, and Thermolysis of Surface-Attached α,ω-Diphenylalkanes. The minimal requirements for a solid to serve as the immobilization support are that it be stable at ~400 °C; that it have reactive surface sites for covalent attachment of the organic moiety of interest; that these sites not be highly catalytically active for hydrocarbon transformations; and that, to gain analytical sensitivity for surface-attached products at low conversion levels, it have moderately high surface areas. These were met by silica, whose surface is terminated by hydroxyl groups which are not strongly acidic. In particular, because of its high purity and convenient physical properties, we chose a fumed silica ("Cabosil") which consists of nonporous, amorphous, spherical primary particles of ~14-nm average diameter, loosely chained together to give ~200 m^2 g^{-1} surface area.[35,36a]

The minimal requirements for the mode of surface attachment are that the covalent link to the surface be stable at ~400 °C; that the position of surface attachment within the organic moiety be somewhat separated from its normal locus of thermal reactivity; and that a facile method for quantitative analysis of surface-attached reactants and products be available. These were met by condensing the surface hydroxyls of silica with phenols to establish a ≡Si—O—C_{ar} linkage, a reaction analogous to the well-known reaction of silica surfaces with alcohols.[35,37] This proved to be an ideal linkage because it is acceptably stable thermally while at the same time being unstable hydrolytically; the latter allowed

Table II. Coverage and Thermal Stability of Surface-Attached α,ω-Diphenylalkanes

ArOH	"saturation coverage"[a] mmol g^{-1} [b]	"saturation coverage"[a] molecules nm^{-2} [c]	ArOH evolved (%), 400 °C, 4 h
PhOH	0.64	2.03	7[d]
15a	0.45	1.46	13[d]
15b	0.43	1.40	32[d]
15c	0.47	1.55	13[e]
15d	0.55	1.85	30[f]

[a] Heating with excess phenol at 220 °C followed by evacuation at 300 °C. [b] Per gram of final product. [c] Based on 200 m^2 g^{-1} of starting silica. [d] No other products detected. [e] Other thermolysis products are the subject of this paper. [f] Other thermolysis products will be the subject of future papers.

(24) The same steady-state analysis allows an estimation of how much **1** is "re-formed" via step −1. The expression for f_{rev}, the fraction of **2** which couples, is $4k_1k_t(W)^2$, where $W = [2(k_1k_t)^{1/2} + k_2(\mathbf{1})^{1/2}]^{-1}$ (see Appendix 1). Inserting the Arrhenius expressions for k_1, k_2, and k_t used in the text at 400 °C and 54 kPa leads to $f_{rev} \simeq 0.1$; in the liquid phase, where (**1**) is much greater, f_{rev} is even smaller. Hence, reversal of C–C homolysis at 400 °C is barely significant. However, a similar calculation at 700 °C and 10 Pa (ref 25) leads to $f_{rev} \simeq 0.999$. This may well explain the "low" values of k_1 obtained at higher temperatures (refs 25 and 26).

(25) Horrex, C.; Miles, S. E. *Discuss. Faraday Soc.* **1951**, *10*, 187.

(26) Sekiguchi, V.; Klabunde, K. J. *Fuel Process. Tech.* **1984**, *4*, 73.

(27) McMillen, D. F.; Ogier, W. C.; Ross, D. S. *J. Org. Chem.* **1981**, *46*, 3322.

(28) Other Arrhenius correlations reported in the liquid phase include $k_1 = 10^{14.4} \exp(-61\,500/RT)$ s^{-1} (ref 16); $k_1 = 10^{15.5} \exp(-63\,000/RT)$ s^{-1} at 6.7 MPa applied pressure (ref 29); and $k_1 = 10^{10.9} \exp(-48\,100/RT)$ s^{-1} (ref 30).

(29) Brower, K. R. *J. Org. Chem.* **1980**, *45*, 1004.

(30) Cronauer, D. C.; Jewell, D. M.; Shah, Y. T.; Kueser, K. A. *Ind. Eng. Chem., Fundam.* **1978**, *17*, 291.

(31) Dunstan, T. D. J., unpublished data.

(32) Thermochemical estimates of k_5, k_{-5}, and k_6 (ref 13) lead to the same inequality.

(33) Vernon, L. W. *Fuel* **1980**, *59*, 102.

(34) Benson, S. W.; Shaw, R. J. *J. Chem. Phys.* **1967**, *47*, 4052.

(35) Iler, R. K. *The Chemistry of Silica*; Wiley: New York, 1979.

(36) (a) Tsuchiya, I. *J. Phys. Chem.* **1982**, *86*, 4107. Ghiotti, G.; Garrane, E.; Morterra, C.; Boccuzzi, F. *Ibid.* **1979**, *83*, 2863. Fripiat, J. J.; Uytterhoeven, J. *Ibid.* **1962**, *66*, 800. The "Aerosil" product used in these studies is made by a process similar to that for the "Cabosil" used herein. (b) Ryason, P. R.; Russell, B. G. *J. Phys. Chem.* **1975**, *79*, 1276. van Roosmalen, A. J.; Mol, J. C. *Ibid.* **1978**, *82*, 2748; **1979**, *83*, 2485.

(37) Azrak, R. G., Angell, C. L. *J. Phys. Chem.* **1973**, *77*, 3048.

for surface detachment subsequent to thermolysis and prior to analysis.

Scouting experiments with phenol showed that surface reaction with silica occurred smoothly at ~200 °C.[38] The standard procedure developed to achieve "saturation coverage" was to disperse an excess of the phenol onto the silica by evaporating solvent from a slurry, to heat the resulting powder at 220 °C in a sealed degassed tube to effect the surface reaction, and to evacuate this product at 300 °C to remove excess phenol. The

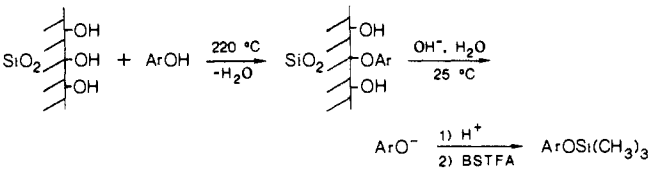

final free-flowing white powder was assayed for the extent of surface coverage and purity by digestion in aqueous base which dissolved the silica and released the surface-attached material as phenoxides. Acidification, extraction, and trimethylsilylation then gave a material suitable for GC and/or GC–MS analysis.

Each of the phenols **15a–d** was attached to silica to provide the surface-immobilized α,ω-diphenylalkanes **16a–d**, which we abbreviate as ~Ph–$(CH_2)_n$Ph. Typical coverage achieved by the

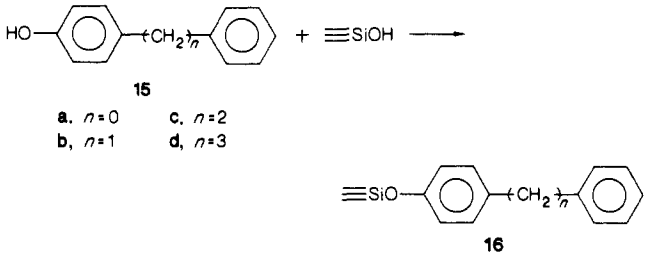

standard procedure was 0.5 mmol g^{-1} (Table II) which, for a silica surface area of 200 m^2 g^{-1}, corresponds to ~1.6 molecules nm^{-2}. Typical dehydrated but not dehydroxylated silicas contain four to five O–H groups nm^{-2}.[35,36,39] Hence, under these forcing conditions, ca. one-third of the surface OH groups have been converted to OAr groups.

Diffuse reflectance Fourier-transform infrared (DRIFT) spectra of the starting silica and of **16c** (0.465 mmol g^{-1}), each as a 10 wt % mixture with KBr, were compared. Each material had been dried but was not rigorously protected from moisture during sample preparation. Characteristic bands occurred in the untreated silica for isolated surface hydroxyls (3741 cm^{-1}), hydrogen-bonded surface hydroxyls (3700–3400 cm^{-1}), and water (3400–3000 cm^{-1}).[36b] Surface attachment of bibenzyl moieties led to loss of the 3741-cm^{-1} band, to a narrowing and intensity decrease of the hydrogen-bonded hydroxyl band normalized to the 1867-cm^{-1} Si–O lattice mode, and to loss of the water band. New bands observed at 3066–2858 and 1609–1450 cm^{-1} are fully consistent with those expected for the bibenzyl moiety. Hence the partial conversion of surface hydroxyl groups to give a more hydrophobic material is clearly revealed by the DRIFT spectrum.

Thermolyses were carried out in sealed degassed Pyrex tubes with a T-shaped configuration such that one arm containing **16** could be inserted into a preheated furnace while the leg was surrounded by a cold trap. Hence volatile products could migrate from the heated zone to the trap as they formed. Heating either surface-attached biphenyl (**16a**) or surface-attached diphenylmethane (**16b**) at 400 °C for 4 h caused evolution of a modest amount of the parent phenols **15a** or **15b** (Table II). We attribute this to slow condensation between surface OAr groups and adjacent residual OH groups to generate ArOH and a surface siloxane linkage. This reaction would be analogous to the well-known dehydroxylation of silica itself[35] which begins to occur in this temperature range. Viewed in the context that biphenyl and diphenylmethane are thermally stable at 400 °C,[23,27,40,41] the more critical observation was that no further products, neither volatile nor surface-attached, were formed for the surface-immobilized analogues **16a** and **16b** either. Thus the mode of surface attachment proved robust enough to retain most of the OAr organic moieties on the surface for periods of hours at 400 °C, and the residual surface OH groups did not catalyze new reaction pathways. In contrast, bibenzyl (**1**) is reactive at 400 °C (Table I), and the extensive set of thermolysis products formed from the surface-attached analogue **16c** forms the nucleus of this paper.

Samples of **16c** with less than "saturation coverage" were prepared similarly except for use of limited amounts of phenol **15c**. We have no explicit evidence at this point whether the OAr groups at limited coverage are uniformly distributed over the surface or whether clustering into "islands" occurs.[42]

Thermolysis of Surface-Attached Bibenzyl (16c). Separate GC and GC/MS analyses were performed on the volatile products collected in the cold trap and the phenolic products formed by basic digestion of the siliceous solid recovered from the heated zone. Thermolyses of **16c** at 350–400 °C at modest conversion levels gave as volatile products, in order of generally decreasing molar amounts: toluene ($PhCH_3$, **3**); ethylbenzene (PhC_2H_5, **11**); benzene (PhH, **10**); bibenzyl ($PhCH_2CH_2Ph$, **1**); styrene (PhC_2H_3, **17**); and stilbene (PhCH=CHPh, **6**). The phenolic products after basic digestion, corresponding to the surface-attached products in parentheses, were even more numerous: *p*-(1-phenylethyl)-phenol (~$PhCHPhCH_3$, **18**); *p*-cresol (~$PhCH_3$, **19**); 9,10-dihydro-3-phenanthrenol (~$PhenH_2$, **20**); 3-phenanthrenol (~Phen, **21**); *p*-ethylphenol (~PhC_2H_5, **22**); phenol (~PhH, **23**); *p*-(*trans*-2-phenylethenyl)phenol (~PhCH=CHPh, **24**); an unidentified isomer of composition $C_{14}H_9OH$ (labeled "~Phen isomer," **25**); a mixture of two isomers of composition $C_{21}H_{19}OH$ which appear to be the two possible para-hydroxylated isomers of 1,2,3-triphenylpropane (labeled ~$PhC_3H_5Ph_2$, **26**); *p*-benzylphenol (~$PhCH_2Ph$, **27**); an isomer of composition $C_{14}H_{11}OH$ which is not *p*-(*cis*-2-phenylethenyl)phenol and is most probably *p*-(1-phenylethenyl)phenol (~$PhCPh{=}CH_2$, **28**); and a mixture of isomeric diphenols (two dominant) of composition $C_{28}H_{24}(OH)_2$ (dehydrodimers of **15c**) (labeled ~$C_{28}H_{24}$~, **29**; see below).

GC analysis of trimethylsilylated phenols from basic digestion of the predominant sample of **16c** (0.465 mmol g^{-1}) used indicated a purity of 99.97%. One trace impurity was 0.018% of the phenol corresponding to **24**, the synthetic precursor of phenol **15c**. Product data were therefore corrected by this amount. A second trace impurity was 0.012% of a mixture of isomeric diphenols (one dominant) also of composition $C_{28}H_{24}(OH)_2$. Their level markedly increased if any oxygen was present during the attachment (220 °C) and evacuation (300 °C) steps of the preparative procedure. However, even with rigorous degassing procedures, this trace level persisted. Subtraction of the GC profiles of the $C_{28}H_{24}(OSiMe_3)_2$ impurities from that of the thermolysis products suggested that only one of the two apparent thermal ~$C_{28}H_{24}$~ products noted above was real; this is the material labeled hereafter as **29**.

Because of the dominance of 1,2,3,4-tetraphenylbutane (**7**) as a fluid-phase thermolysis product of **1** (Table I), the doubly hydroxylated tetraphenylbutanes ($C_{28}H_{24}(OH)_2$), which would correspond to analogous surface-attached dehydrodimers, were synthesized. Coupling of *p*-methoxyethylbenzene at the benzylic carbon with di-*tert*-butyl peroxide has been described by Anderson et al.[43] Application of this procedure to *p*-methoxybibenzyl (**30**) gave a mixture of isomers **31a–c** (two diastereoisomers are possible

(38) Stotfeldt-Ellingsen, D.; Resing, H. A. [*J. Phys. Chem.* **1980**, *84*, 2204] report ≡SiOPh with no preparative details.
(39) Sindorf, D. W.; Maciel, G. E. *J. Phys. Chem.* **1982**, *86*, 5208.
(40) Allen, G. T.; Gavalas, G. R. *Fuel* **1984**, *63*, 586.
(41) Benjamin, B. M.; Raaen, V. F.; Maupin, P. H.; Brown, L. L.; Collins, C. J. *Fuel* **1978**, *57*, 269.
(42) Examples of both situations have been claimed, e.g.: Hall, L. D.; Waterton, J. C. *J. Am. Chem. Soc.* **1979**, *101*, 3697. Lochmuller, C. H.; Colborn, A. S.; Hunnicutt, M. L.; Harrison, J. M. *Anal. Chem.* **1983**, *55*, 1344.
(43) Anderson, R. A.; Dalgleish, D. T.; Nonhebel, D. C.; Pauson, P. L. *J. Chem. Res. (M)* **1977**, 227.

Table III. Products from Thermolysis of ~~$PhCH_2CH_2Ph$ at 0.465 mmol g^{-1} Coverage

temp (°C)	400	400	400	375	375	375	375	375	350	350
time (min)	10	30	90	10	20	40	60	600	20	180
charge (mmol)	0.136	0.154	0.149	0.241	0.124	0.126	0.157	0.104	0.180	0.162
~~$PhCH_2CH_2Ph$ (mol, rel)										
charged	100	100	100	100	100	100	100	100	100	100
evolved	5.4	13.1	11.4	6.1	5.7	5.0	5.3	8.5	5.3	6.8
unreacted	90.2	81.1	62.5	94.9	93.6	92.1	89.8	59.3	94.5	89.1
consumed	4.4	5.8	26.1	−1.0	0.7	2.9	4.9	32.2	0.2	4.1
products formed										
equiv, rel	4.2	10.3	21.1	0.45	1.6	3.3	5.3	28.3	0.16	2.4
mol, rel	4.7	12.4	26.7	0.52	1.8	3.7	5.9	34.9	0.19	2.6
product distribution (mol %)										
~~$PhCH_3$ (**19**)	7.5	10.7	14.8	10.8	6.9	6.1	6.6	10.7	10.7[d]	5.6
$PhCH_3$ (**3**)	5.9	7.6	11.4	10.5	5.4	5.3	4.8	10.6	10.8	5.2
$PhCH_2CH_2Ph$ (**1**)	1.0	1.5	1.5	0.6	0.4	0.8	0.8	1.2	*c*	1.0
~~$PhC_3H_5Ph_2$ (**26**)	1.1	0.7	0.7	1.2	0.9	0.8	0.6	0.2	1.5	0.5
~~PhCH=CHPh (**24**)	4.1	4.2	2.1	8.0	4.1	3.3	3.0	1.9	10.4	2.5
PhCH=CHPh (**6**)	0.3	0.5	0.9	0.3	0.2	0.2	0.2	0.6	1.0	0.1
~~$PhCHPhCH_3$ (**18**)	57.9	48.3	38.6	51.5	65.2	62.9	62.7	43.1	48.4	66.8
~~$PhCH_2Ph$ (**27**)	0.5	1.5	3.8	*c*	0.3	0.4	0.6	2.9	*c*	0.6
~~$PhCPh{=}CH_2$ (**28**)	0.5	0.4	0.6	1.3	0.5	0.3	0.5	0.7	*c*	0.4
~~$PhenH_2$ (**20**)	4.5	1.8	0.8	6.1	6.1	4.6	3.5	0.6	5.0	4.6
~~Phen (**21**)	4.0	5.0	6.6	0.7	2.1	3.4	4.7	8.8	*c*	2.5
~~Phen isomer (**25**)	0.7	1.0	1.3	0.3	0.4	0.6	0.8	1.7	*c*	0.5
~~PhC_2H_5 (**22**)	3.2	3.9	4.3	1.7	2.4	2.9	3.0	4.4	1.3	2.4
PhH (**10**)	2.3	2.2	2.7	2.4	1.2[a]	2.1	2.1	3.6	3.3[a]	2.0
~~PhH (**23**)	2.4	6.3[a]	3.9	1.8	2.0	2.3	2.6	3.5	1.8	2.6
PhC_2H_5 (**11**)	2.9	2.6	2.8	1.9	1.1[a]	2.6	2.4	3.6	1.5	2.1
PhC_2H_3 (**17**)	0.8	1.9	2.7	0.4	0.4[a]	0.6	0.6	1.7	*c*	0.4
~~$C_{28}H_{24}$~~ (**29**)	0.4	*b*	*b*	0.4	0.6	0.7	0.5	0.1	*c*	0.4

[a] Possible outliers based on patterns shown in Figure 2. [b] Not analyzed. [c] Below detection limit. [d] Column normalized to 96 mol % to account for products below detection limit; values probably only accurate to one significant place.

for each; five isomers were resolvable by GC; see Experimental Section). Demethylation gave the desired phenols **32a–c** which

$$\underset{\mathbf{30}}{AnCH_2CH_2Ph} \xrightarrow[140\ °C]{(t\text{-}BuO\text{-})_2} \underset{\mathbf{31a}}{(PhCH_2CHAn\text{-})_2} + \underset{\mathbf{31b}}{(AnCH_2CHPh\text{-})_2} + \underset{\mathbf{31c}}{PhCH_2CHAnCHPhCH_2An}$$

[An = *p*-$CH_3OC_6H_4$–]

were trimethylsilylated for GC analysis. The minor thermal product **29** does not appear to correspond to any one of these authentic benzylically coupled dehydrodimers nor to the major oxidative impurity, and its exact identity remains unknown. More importantly, the availability of **32a–c** allowed setting a very low upper limit on the occurrence of the surface-attached analogue of radical coupling step 4 (see below).

Data for the 18 products detected from thermolysis of **16c** at the highest coverage used (0.465 mmol g^{-1}) are compiled in Table III for runs at 400 °C (4.2–21.1% conversion), 375 °C (0.45–28.3% conversion), and 350 °C (0.16–2.4% conversion). The amount of surface-attached bibenzyl moieties charged to the reaction tube is listed in row 3 in units of mmol. This is then expressed in row 4 as 100 relative molar units as the comparative standard for rows 5–9. Row 5, "~~$PhCH_2CH_2Ph$ evolved", is the small amount of phenol **15c** recovered from the cold trap. Row 6, "~~$PhCH_2CH_2Ph$ unreacted", is the amount of **15c** recovered from basic digestion of the siliceous residue after reaction. Row 7, "~~$PhCH_2CH_2Ph$ consumed", is then the difference between "~~$PhCH_2CH_2Ph$ charged" and the sum of "~~$PhCH_2CH_2Ph$ evolved" and "~~$PhCH_2CH_2Ph$ unreacted". Row 9, "products formed, mol", is the molar sum of all products detected; in row 8, "products formed, equiv", this sum has been converted to a common C_{14} basis. For ideal material balance, rows 7 and 8 should be equal. Because the former suffers from being a small difference between two or more large numbers determined in nonparallel fashion, we consider the latter as much the more reliable measure of conversion. The product distributions (rows 10 ff) are expressed as molar selectivities normalized to 100% for all detected products.

The noncondensable gas formed during a run at ~400 °C which achieved ~20% conversion (comparable to the 400 °C–90 min entry in Table III but not included there because of less precise temperature control and less complete product analysis) was measured manometrically. It was predominantly hydrogen ($H_2/CH_4 > 8$) by mass spectroscopy. Relevant molar ratios were H_2:**21**:**20**:**10**:**22**:**11**:**23** = 1:1.00:0.10:0.31:0.38:0.34:0.31. Hence, of the hydrogen atoms potentially made available by cyclization of **16c** to form **20** and **21** {2(**20**) + 4(**21**) = 4.2 in these relative units}, 32% was accounted for in the C_6 and C_8 unsymmetrical

Table IV. Products from Thermolysis of ~~$PhCH_2CH_2Ph$ As a Function of Coverage

temp (°C)	400[a]	400	375[a]	375
time (min)	90	90	60	60
coverage (mol g^{-1})	0.465	0.104	0.465	0.158
charge (mmol)	0.149	0.047	0.157	0.095
~~$PhCH_2CH_2Ph$ (mol, rel)				
charged	100	100	100	100
evolved	11.4	19.3	5.3	7.5
unreacted	62.5	70.4	89.8	95.2
consumed	26.1	10.3	4.8	−2.7
products formed				
equiv, rel	21.1	12.4	5.3	2.3
mol, rel	26.7	17.0	5.9	2.9
product distribution (mol %)				
~~$PhCH_3$ (**19**)	14.8	19.1	6.6	14.6
$PhCH_3$ (**3**)	11.4	15.6	4.8	11.5
$PhCH_2CH_2Ph$ (**1**)	1.5	1.5	0.8	0.8
~~$PhC_3H_5Ph_2$ (**26**)	0.7	0.8	0.6	2.5
~~PhCH=CHPh (**24**)	2.1	2.9	3.0	6.4
PhCH=CHPh (**6**)	0.9	1.0	0.2	*c*
~~$PhCHPhCH_3$ (**18**)	38.6	25.0	62.7	41.5
~~$PhCH_2Ph$ (**27**)	3.8	1.6	0.6	0.6
~~$PhCPh{=}CH_2$ (**28**)	0.6	0.9	0.5	0.5
~~$PhenH_2$ (**20**)	0.8	5.2	3.5	7.5
~~Phen (**21**)	6.6	4.2	4.7	1.4
~~Phen isomer (**25**)	1.3	0.9	0.8	0.4
~~PhC_2H_5 (**22**)	4.3	4.6	3.0	2.9
PhH (**10**)	2.7	5.0	2.1	3.2
~~PhH (**23**)	3.9	4.9	2.6	2.9
PhC_2H_5 (**11**)	2.8	3.5	2.4	2.6
PhC_2H_3 (**17**)	2.7	3.2	0.6	0.9
~~$C_{28}H_{24}$~~ (**29**)	*b*	*b*	0.5	*c*

[a] From Table III. [b] Not analyzed. [c] Below detection limit.

Table V. C, H Balance in Thermolysis Products from ~~$PhCH_2CH_2Ph$

conditions	conversion (%)	C found[a-c]	H found[a-d]	H expected[a,e]	H deficiency[a,f]	H deficiency (%)[g,h]
375 °C; 20 min; 0.465 mmol g^{-1}	1.6	22.78	20.91	21.15	0.24	1.1
375 °C; 60 min; 0.158 mmol g^{-1}	2.3	32.77	30.48	30.43	−0.05	−0.2
350 °C; 180 min; 0.465 mmol g^{-1}	2.4	33.43	30.91	31.04	0.13	0.4
375 °C; 40 min; 0.465 mmol g^{-1}	3.3	46.67	42.99	43.34	0.35	0.8
400 °C; 10 min; 0.465 mmol g^{-1}	4.2	58.47	53.81	54.30	0.49	0.9
375 °C; 60 min; 0.465 mmol g^{-1}	5.3	73.94	67.89	68.66	0.77	1.1
						av 0.7 ± 0.5

[a] Mol relative to 100 mol ~~$PhCH_2CH_2Ph$ (i.e., 1400 mol C and 1300 mol H) charged. [b] Summation of all products (Tables III and IV). [c] 1 equiv CH_4 assumed for each equiv ~~$PhCH_2Ph$ formed. [d] 1 equiv surface OH assumed for each equiv $PhCH_2CH_2Ph$ and PhCH = CHPh formed. [e] (C found) × (13/14). [f] Hydrogen deficiency = (H expected) − (H found). [g] (H deficiency)/(H expected) × 100%. [h] Molecular hydrogen not included.

hydrogenolysis products {(**10**) + (**22**) + (**11**) + (**23**) = 1.34} and 48% as molecular hydrogen.

Analogous data at lower coverages (Table IV) consist of a 4.5-fold variation in coverage at 400 °C and a 2.9-fold variation at 375 °C.

As a control experiment, bibenzyl, largely in the liquid state, was heated at 400 °C for 90 min with and without the addition of 45 wt % dried silica. The observed product distributions[12] were indistinguishable within experimental error. Hence there is no effect of the silica when the bibenzyl moiety is not covalently attached.

Discussion

Thermolysis of surface-attached bibenzyl (**16c**) (Table III) is accelerated about fourfold compared with that of fluid bibenzyl (**1**) (Table I). In addition, surface attachment leads to major changes in product distributions: (1) the virtual disappearance of dehydrodimers (~~$Ph(-C_4H_6Ph_2-)Ph$~~ vs. **7**); (2) the marked increase in rearrangement (~~$PhCHPhCH_3$ vs. **9**) to the point where it has become the major reaction pathway; and (3) the emergence of both cyclization to form phenanthrene derivatives (~~$PhenH_2$ and ~~Phen) and unsymmetrical cleavage to form C_6 and C_8 products from being barely detectable to being stoichiometrically significant. Thus, to the initial question posed: "Does surface immobilization change thermal reactivity in a nontrivial manner?", we can clearly answer: "Yes". We now explore possible mechanistic factors underlying these changes. However, because of our currently limited structural information about the surface-attached "state", many of our comments will be more akin to hypotheses and suggestions for further work than firm conclusions.

Nature of the Surface Layer. What is the spatial relationship between nearest bibenzyl neighbors at the "saturation coverage" of 0.465 mmol g^{-1} (1.55 molecules nm^{-2}) (Table II)? Because of uncertainties involving the local surface structure of amorphous silica, such as the exact placement of OH groups with respect to each other and the angles with which the Si–O bonds emerge from the surface, only an approximate but nevertheless revealing answer can be given. Consider as idealized models the low-index surfaces of crystalline silicas, such as β-cristobalite,[39] and an attached phenyl group with its $O-C_1-C_4$ axis normal to the surface (**33a**).

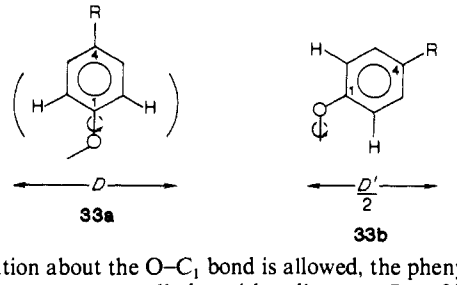

33a **33b**

If free rotation about the $O-C_1$ bond is allowed, the phenyl group would then sweep out a cylinder with a diameter $D \simeq 2[d_{CC}(\sin 60°) + d_{CH}(\sin 60°) + r_{H,\ van\ der\ Waals}] \simeq 2[(0.140)(0.87) + (0.108)(0.87) + (0.12)] \simeq 0.67$ nm.[44] The (111) surface has 4.55 single OH groups nm^{-2} placed 0.50 nm apart in a hexagonal array. Cylinders of $D \simeq 0.67$ nm could occupy only every third OH site without serious steric interference. This model thus predicts a maximum coverage of (4.55/3) = 1.52 nm^{-2} and a center-to-center distance of 0.87 nm between occupied sites. The (100) surface has 3.95 geminal OH sites nm^{-2} placed 0.50 nm apart in a square array. It could accommodate cylinders of $D \simeq 0.67$ nm on every second site for a maximum coverage of 1.98 nm^{-2} and a center-to-center distance of 0.71 nm. Comparing these simplified models with our observed "saturation coverage" of 1.55 nm^{-2} for **16c**, we picture a two-dimensional layer of anchored organic moieties quite close to each other but with enough room for considerable conformational mobility by bond rotations, i.e., a "liquid-like" monolayer.

The idealized model **33a** with the $O-C_1-C_4$ axis normal to the surface implies that the Si–O bond emerges from the surface at an acute angle to compensate for the Si–O–C angle (120–130°).[45] If in the other extreme the Si–O bond were normal to the surface and if free rotation were allowed about it (**33b**), the phenyl ring would sweep out a cylinder of much larger diameter D'. Thus, the observed coverage could only be achieved at the expense of full rotational freedom about the Si–O bond. We will see below when considering the probability of bimolecular reactions between adjacent surface-attached species that the distribution of angles which the $O-C_1-C_4$ axis makes with the surface is a critical variable. More knowledge of detailed surface geometry is needed.[38]

C, H Material Balance. Considering the rarity of attempting to deal quantitatively with an organic reaction producing as many as 18 products, we first examine the C, H material balance as a measure of internal consistency of the data. Note that most of the products do have H:C ratios different from those of **16c**. As a compromise between analytical sensitivity and minimal complication from secondary reactions, we treat in Table V the six runs in the conversion range 1.6–5.3%. A slight deficiency of H compared with C appears in the cumulative products, only 0.7 ± 0.5% overall and 0.9 ± 0.3% for the high coverage runs. However, if H_2 is produced in the same proportions in all runs as in the one run where it was quantified (see above), then even this small deficiency disappears. Hence, material balance is excellent.

C–C Homolysis. Homolysis of **16c** via step 1a would be expected to form a surface-attached benzyl radical (**34**) and a benzyl radical (**2**) "free" within the porosity of the solid. The distinctive product formed from **34** is clearly ~~$PhCH_3$ (**19**), while "free"

~~$PhCH_2CH_2Ph$ (**16c**) → ~~$PhCH_2\cdot$ (**34**) + $\cdot CH_2Ph$ (**2**) (1a)

benzyl fragments are found as toluene (**3**) and, to a lesser extent, as part of ~~$PhC_3H_5Ph_2$ (**26**). The source of the small amount of bibenzyl (**1**) product is ambiguous. It may have been formed from coupling of **2** or from hydrogenolytic cleavage of the ≡SiO—$PhCH_2CH_2Ph$ bond in a process parallel to the unsymmetrical hydrogenolysis process which gives C_6 and C_8 products

(44) *CRC Handbook of Chemistry and Physics*, 58th ed.; CRC Press: Cleveland, 1977.

(45) Si–O–C angles would be expected to fall in the range 120–130°; e.g.: Kanters, J. A.; van Veen, A. M. *Cryst. Struct. Commun.* **1973**, *12*, 261. Si–O–Si angles in crystalline silicas are typically 145–155°; *Gmelins Handbuch der Anorganischen Chemie*; Verlag Chemie: Weinheim, 1959; Vol. 15B.

Table VI. Product Relationships as a Function of Conversion Level and Coverage

conversion (%)	T (°C)	t (min)	coverage (mmol g^{-1})	surface C_7 products/ free C_7 products	ΣC_7's/ Σterm	(27)/ (18)	(28)/ [(18) + (27)]	(22)/ (10)	[(11) + (17)]/ (23)	[(22) + (10)]/ [(11) + (17) + (23)]
0.16	350	20	0.465	0.87	0.89	*b*	*c*	0.4[d]	0.8	1.4[d]
0.45	375	10	0.465	0.92	0.97	*b*	0.023	0.7	1.3	1.0
1.6	375	20	0.465	1.09	0.99	0.005	0.008	2.0[d]	0.8[d]	1.0[d]
2.4	350	180	0.465	0.98	1.31	0.009	0.006	1.2	1.0	0.9
3.4	375	40	0.465	1.00	1.03	0.006	0.005	1.4	1.4	0.9
4.2	400	10	0.465	1.07	1.01	0.009	0.009	1.4	1.5	0.9
5.3	375	60	0.465	1.22	1.11	0.010	0.008	1.4	1.2	0.9
10.3	400	30	0.465	1.29	1.23[a]	0.031	0.008	1.8	0.7[d]	0.6[d]
21.1	400	90	0.465	1.22	1.92[a]	0.098	0.014	1.6	1.4	0.7
28.4	375	600	0.465	0.99	2.07	0.068	0.015	1.2	1.5	0.9
2.3	375	60	0.158	1.04	1.39	0.014	0.012	0.9	1.2	1.0
12.4	400	90	0.104	1.16	2.02	0.064	0.034	0.9	1.4	0.8
			av	1.07 ± 0.12				1.3 ± 0.3	1.3 ± 0.2	0.9 ± 0.1

[a] ~~$C_{28}H_{24}$~~ not measured. [b] **27** below detection limit. [c] **28** below detection limit. [d] Omitted from average because of one or more apparent outliers (Figure 2).

Table VII. Rate Constants for Homolysis (k_{1a}) and Total Disappearance (k_T) of ~~$PhCH_2CH_2Ph$~~

T (°C)	t_{exptl} (min)	coverage (mmol g^{-1})	conversion (%)	$k_T \times 10^6$ (s^{-1})[a]	$k_{1a} \times 10^6$ (s^{-1})[b]
400	10	0.465	4.2	81	6.6
	30	0.465	10.3	67	7.6
	90	0.465	21.1	47	8.1
	90	0.104	12.4	27.5	6.8
					av 7.3 ± 0.6
375	10	0.465	0.45	8.6	1.12
	20	0.465	1.6	14.8	1.07
	40	0.465	3.4	14.8	1.01
	60	0.465	5.3	15.8	1.06
	600	0.465	28.4	9.7	1.29
	60	0.158	2.3	7.0	1.21
					av 1.13 ± 0.10
350	20	0.465	0.16	1.43	0.20
	180	0.465	2.4	2.33	0.15
					av 0.17_5 ± 0.03

[a] First-order dependence is formal only. [b] First-order behavior is assumed.

(see below). Thermolysis of silica covered with a mixture of bibenzyl and biphenyl moieties (prepared from a mixture of **15c** and **15a**) gave small amounts of both bibenzyl and biphenyl;[31] however, thermolysis of **16a** did not produce biphenyl. Therefore, we tentatively assign bibenzyl (and biphenyl) formation as a hydrogenolysis process, dependent on homolysis of ~~$PhCH_2CH_2Ph$~~ for its initiation (see below). We then define the ratio "surface C_7 products: free C_7 products" as (**19**)/[(**3**) + (**26**)]. It shows no obvious trend with conversion level or coverage (Table VI) and has an average value of 1.07 ± 0.12 (1.02 ± 0.11 for the runs with ≤5.3% conversion), not signficantly different from the ideal value of 1.00. Therefore, we conclude that we have correctly defined the major fates of C_7 radicals **2** and **34**, and we define "ΣC_7's" as [(**3**) + (**19**) + (**26**)].

Is the rate of homolysis step (1a) affected by surface immobilization? Product evolution vs. time plots are shown in Figure 1 for the most extensive data at one temperature and coverage (375 °C; 0.465 mmol g^{-1}). For such limited conversion levels of ≲5%, such plots will, of course, show negligible curvature, regardless of the exact kinetic order. The plot for ΣC_7's is indeed effectively linear with a least-squares slope of 0.0117 mol % min^{-1} (r^2 = 0.999). The time axis intercept of 0.2 min is not inconsistent with our independent experimental estimates of heatup and cooldown times. A *formal* first-order rate constant for total disappearance of **16c**, k_T, can be calculated at each data point from:

$$k_T = \left(\frac{1}{t}\right) \ln \frac{(\mathbf{16c})_0}{(\mathbf{16c})_f} = \left(\frac{1}{t}\right) \ln \frac{(\mathbf{16c})_0}{[(\mathbf{16c})_0 - (\Sigma\text{products})]}$$

To account for the small amount of phenol **15c** evolved (E) during the reaction (Tables III and IV) which slightly changes the effective starting concentration of **16c**, we take $(\mathbf{16c})_0 = 100 - (E/2)$; ($\Sigma$products) is expressed as C_{14} equivalents in units of mol/100 mol of **16c**; we take $t = (t_{exptl} - 1)$ min to account for the short heatup period. The rate constant for homolysis, k_{1a}, can then be obtained from:

$$k_{1a} = f_{C_7's}(k_T)$$

where $f_{C_7's}$ is the fraction of **16c** converted to C_7's on a C_{14} equivalents basis. Values of k_T and k_{1a} are compiled in Table VII.

The values of k_T at high coverage first increase with increasing conversion (most obvious at 350 °C and the early values at 375 °C) and then decrease (most obvious at 400 °C). They decrease with decreasing coverage when comparisons are made at similar conversion levels. Hence, the overall disappearance of **16c** is clearly not first-order. Yet, the derived values of k_{1a} appear independent of both conversion level and coverage, indicative of the first-order behavior expected for C–C homolysis. Arrhenius treatment of the twelve values of k_{1a} in Table VII leads to E = 62.9 ± 1.8 kcal mol^{-1} and $A = 10^{(15.3\pm0.6)}$ s^{-1} (r^2 = 0.992). The homolysis rate constants for gaseous, liquid (tetralin), and surface-attached bibenzyl at 375 °C are thus 2.2×10^{-6},[15,16] 1.1×10^{-6},[15,27] and 1.2×10^{-6} s^{-1}, respectively. To be precise, a better fluid-phase model for ~~$PhCH_2CH_2Ph$~~ would be bibenzyl bearing a para oxy substituent. However, such a substituent effect would be expected to be small.[46] Hence, within the certainties of comparing exact values of rate constants and Arrhenius parameters

(46) Creary, X. *J. Org. Chem.* **1980**, *45*, 280. A *p*-hydroxyl substituent gave a 1.7-fold acceleration at 100 °C in the rate-controlling generation of a benzylic radical by homolysis of the strained C–C bond in 2,2-dimethyl-3-aryl-1-methylenecyclopropanes. If this effect is assumed to be enthalpic, the acceleration at 375 °C would be only 1.4-fold.

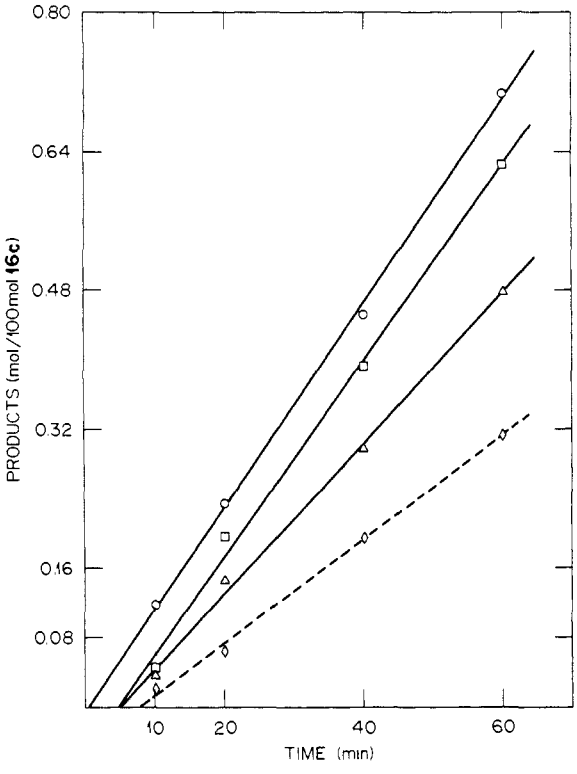

Figure 1. Product evolution profiles for thermolysis of surface-attached bibenzyl (**16c**; 0.465 mmol g^{-1}); 375 °C: O, ΣC_7's; □, Σrearr (÷6); △, Σcycl; ◇ Σ(unsym cleav/2).

from separate investigators, we conclude that surface attachment has not fundamentally altered the initial C–C homolysis step.

Hydrogen Atom Transfer and Induced Decomposition. The several C_{14} products observed suggest hydrogen abstraction from **16c** in an analogue of step 2. It is not surprising that the "free" benzyl radical produced in step 1a should react via step 2a to

$$\underset{\mathbf{2}}{PhCH_2\cdot} + \underset{\mathbf{16c}}{\sim\!PhCH_2CH_2Ph} \rightarrow \underset{\mathbf{3}}{PhCH_3} + \underset{\mathbf{35}}{\sim\!PhCH_2\dot{C}HPh} \quad (2a)$$

$$\underset{\mathbf{34}}{\sim\!PhCH_2\cdot} + \mathbf{16c} \rightarrow \underset{\mathbf{19}}{\sim\!PhCH_3} + \mathbf{35} \quad (2b)$$

produce surface-attached radical **35** (for convenience, we write only one of the possible positional isomers of **35** whereas both are presumably produced in an as yet unknown ratio). The results indicate that indeed much of the surface-attached analogue **34** reacts similarly. Hence, there must be enough conformational mobility of surface-attached species **16c** and **34** to allow the oriented encounter between nearest neighbors needed for hydrogen atom transfer in step 2b. Consideration of molecular models suggests that the (currently unknown) distribution of angles between the O–C_1–C_4 axis and the surface (see **33**) is a critical parameter in determining the probability of such encounters.

Decay products from radical **35**, not involving rearrangement or cyclization (see below), appear to be ~PhCH=CHPh (**24**), the trace of PhCH=CHPh which may arise from secondary reaction of **24**, ~$PhC_3H_5Ph_2$ (**26**), and possibly the trace of dehydrodimer **29** (whose exact structure remains unknown). The dramatic change from fluid-phase results (Table I) is the reduction in formation of coupling products **26** (~1 mol %) and **29** (≲0.5 mol %) compared with **5** and **7**. This appears to be a direct result of surface immobilization which prevents free diffusion of **35**. In the rare occasions when two immobilized radicals might find themselves on adjacent surface sites, there is no reason to believe that the combination:disproportionation ratio in step 4a might not be lower than in solution (step 4), especially if disproportionation requires less intimate contact. Yet **24** is never more than a minor product, either.

The number of radicals formed by homolysis must equal the number destroyed in radical–radical encounters. Including both

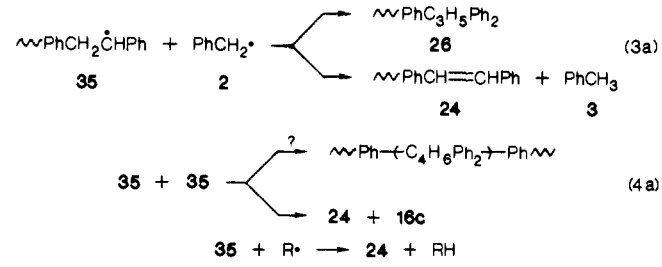

probable combination and disproportionation products, we define Σterm = 2[(**24**) + (**6**) + (**28**) + (**17**) + (**26**) + (**29**)]. At low conversions and high coverage, the ratio ΣC_7's:Σterm is indeed close to the ideal value of I (Table VI). However, at lower coverages, it exceeds unity for reasons not yet understood. In this exercise, we have not specified which "saturated products" accompany the olefinic disproportionation products included in the Σterm. However, the implication is that significant quantities of $PhCH_3$ and PhC_2H_5, for example, may be formed by disproportionation events as well as by hydrogen atom transfer.

Rearrangement. We turn next to the major product, ~$PhCHPhCH_3$ (**18**), and the traces of ~$PhCH_2Ph$ (**27**) and ~$PhCPh{=}CH_2$ (**28**). Since the ratio of **27**:**18** approaches zero at zero conversion (Table VI), **27** must result from secondary decomposition of **18**. The ratio of **28**:(**18** + **27**), while always very small and subject to scatter, shows no obvious trend with conversion (Table VI); **28** is thus most likely a primary disproportionation product. We define Σrearr as [(**18**) + (**27**) + (**28**)]. These rearranged products suggest the occurrence of a chain sequence, steps 5a and 6a, analogous to fluid-phase behavior. Again a hydrogen atom transfer (step 6a) must proceed smoothly between nearest surface-attached neighbors, in this case, rearranged radical **36** and substrate **16c**.

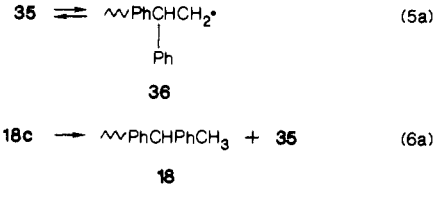

The linearized time evolution plot of Σrearr at 375 °C at low conversions (0.0677 mol % min^{-1}; r^2 = 0.996; Figure 1) has a time intercept of 4.6 min, notably longer than that for ΣC_7's. This difference is displayed in a different format in Figure 2 where product selectivities are plotted against conversion level. [In Figure 2, data at 350, 375, and 400 °C are plotted together (although separately identified) because selectivities appear more sensitive to conversion level than to temperature for the range of each variable being considered.] The unusual feature of Figure 2 is the maximum in selectivity for Σrearr and the corresponding minima in selectivity for ΣC_7's and Σterm which occur at the very low conversion level of only 2–3%. Such extrema suggest at least two opposing effects of conversion level which need to be unraveled.

The longer time intercept for Σrearr than for ΣC_7's in Figure 1 and the related behavior to the left of the extrema in Figure 2 suggest a short "inhibition period" before the rate of formation of rearranged products becomes "normal". Noting the chain character of rearrangement (steps 5a and 6a), we propose that the simplest explanation is a trace of some unidentified chain inhibitor. This transitory effect should not, however, be overemphasized since its effective period of ~4 min (Figure 1) corresponds to only [0.0117 mol % ΣC_7's min^{-1})/2](4 min) = 0.023 mol % homolysis of **16c** and is revealed only because of the collection of data at extremely low conversions.

We define L'_{rearr} = Σrearr/ΣC_7's, analogous to our earlier definition of L_{rearr} = (**9**)/(**3**) in the liquid phase. However, to the extent that some of the C_7 products **3** and **19** are formed by disproportionation (see above) rather than by hydrogen atom transfer from **16c** to generate **35**, L'_{rearr} is a lower limit for the chain length for rearrangement in the surface-attached case. Determining the inherent initial value of L'_{rearr} at high coverage

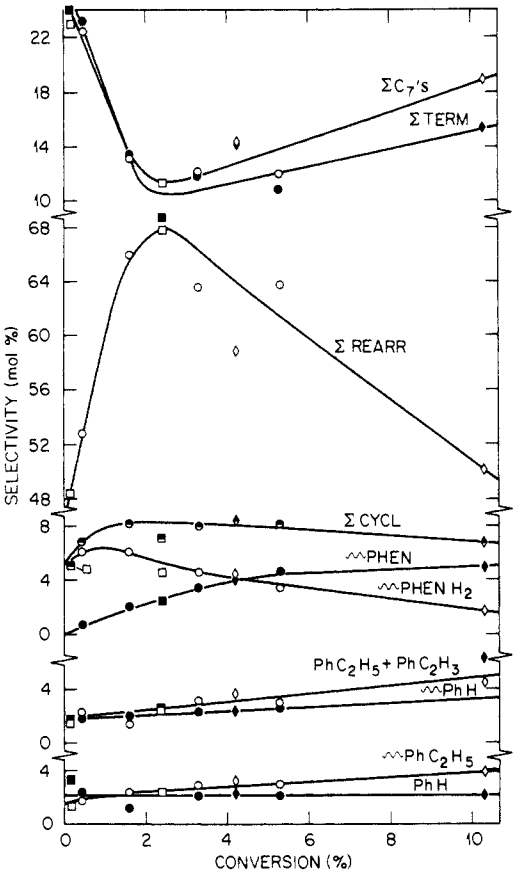

Figure 2. Product selectivity patterns as a function of conversion level for thermolysis of surface-attached bibenzyl (**16c**; 0.465 mmol g^{-1}): □, 350 °C; ○, 375 °C; ◇, 400 °C. Starting from the top: open symbols (ΣC_7's) and filled symbols (Σterm); open symbols (Σrearr); half-filled symbols (Σcycl), open symbols (〰$PhenH_2$), and filled symbols (〰Phen); open symbols (PhC_2H_5 plus PhC_2H_3) and filled symbols (〰PhH); open symbols (〰PhC_2H_5) and filled symbols (PhH).

is not straightforward because it is suppressed during the short inhibition period at very low conversions, reaches a maximum shortly thereafter, and then decreases again at higher conversions. This latter dependence can be seen in the behavior to the right of the extrema in Figure 2. At 375 °C, we take the slopes of the linear portions of the product evolution curves in Figure 1 as indicative of inherent initial behavior after the brief inhibitory disturbance is over but before downward curvature beings (extension of Figure 1 to the 600-min point would lead to marked downward curvature for Σrearr). This ratio of slopes gives $L'_{rearr}{}^{375°C} = (0.0677)/(0.0117) = 5.8$ (Table VIII). Having only two low-conversion points at 350 °C, we resort to a linear connection between them to obtain $L'_{rearr}{}^{350°C} \simeq 6.7$. The use of initial slopes at 400 °C is not possible because the data points were necessarily taken at considerably higher (albeit still modest) conversions because times <10 min would have been seriously perturbed by heatup and cooldown. Product evolution vs. time curves for Σrearr (not pictured) curve downward already at the 10-min point such that estimation of the tangent at zero time is quite arbitrary. Hence, we resort to extrapolation of selectivity vs. conversion plots (not pictured but analogous to Figure 2) to zero conversion; note that the 400 °C data set is not affected significantly by the inhibition period which is already long over at the first data point. These "zero-conversion" intercepts give $L'_{rearr}{}^{400°C} = (61.3)/(11.1) = 5.5$. The values of L'_{rearr}, compiled in Table VIII, decrease slightly with increasing temperature. However, in light of the varying data reduction procedures used at the various temperatures, this trend may well not be statistically significant.

Why has L'_{rearr} for the surface-attached state increased at least 30-fold compared with L_{rearr} for the neat liquid (Table I)? As a point of reference, we can write a *formal* expression for L'_{rearr} analogous to that developed explicitly for the liquid phase (see above):

$$L'_{rearr} \simeq \left(\frac{1}{2}\right)\left(\frac{1}{k_{1a}k_{ta}}\right)^{1/2} K_{5a}k_{6a}(\mathbf{16c})^{1/2}$$

where k_{ta} represents the termination events. The extension from fluids to the surface-attached condition for unimolecular elementary steps, such as k_{1a}, k_{5a}, and k_{-5a}, does not appear particularly troublesome. However, for bimolecular elementary steps such as k_{4a} and k_{6a}, it is not immediately obvious how to define rate constants and "concentrations". The kinetic driving force for a surface-attached species to react with a neighbor will not be its "concentration" in any global sense, nor even its "surface coverage", so long as it cannot freely migrate on the surface. It will presumably depend in some inverse fashion on the distance between the sites of attachment modified by a weighted average over all relative conformations achievable by bond rotations (see above) of the reacting species. More research will be needed to formulate this problem clearly. Nevertheless, we find this formal expression for L'_{rearr} useful to illustrate our current suggestion that the large increase in the chain length for rearrangement which accompanies surface immobilization results predominantly from a large effective decrease in "k_{ta}" for radical termination. The hydrogen atom transfer step (6a) (in the numerator) may, in fact, be inherently somewhat slower, even for nearest neighbors on the surface, than in the neat liquid. However, this decrease would be more than offset by a much greater decrease in the rate of radical termination (in the denominator). This conclusion drawn from L'_{rearr} is reinforced by the large decrease in formation of radical coupling products already discussed above.

Table VIII. Dependence of L' Values on Reaction Conditions

	L'_{rearr}	L'_{cycl}
Variation with Temperature at High Coverage (0.465 mmol g^{-1}) and "Zero" Conversion		
T (°C)		
350	6.7	0.70
375	5.8	0.74
400	5.5	0.72
Variation with Conversion at 400 °C and High Coverage (0.465 mmol g^{-1})		
conv (%)		
0	5.5	0.72
4.2	4.1	0.59
10.3	2.6	0.36
21.1	1.6	0.28
Variation with Coverage at 375 °C and 60 min		
coverage (mmol g^{-1}) conv (%)		
0.465	5.3	0.68
0.158	2.3	1.5	0.31

The value of $L'_{rearr}{}^{400°C}$ at high coverage calculated from the *cumulative* products at progressively longer reaction times decreased (Table VIII) to only 30% of its initial value at only 20% conversion. A similar decrease in the value of L'_{rearr} with decreasing initial coverage at low conversion levels is seen most clearly in the 375 °C–60 min data set (Table VIII). Both these decreases probably result from a decrease in the rate of step 6a as it becomes more and more difficult for the rearranged surface-attached radical **36** to "find" a neighboring molecule of surface-attached **16c** at an accessible distance and in a favorable conformation to transfer a hydrogen atom. However, in light of the ambiguity of defining the relevant kinetic terms, we refrain from further speculation at this time.

Cyclization. The compensating selectivity-vs.-conversion behavior for 〰$PhenH_2$ (**20**) and 〰Phen (**21**) (Figure 2) shows that **20** is formed initially with **21** being derived from it. We therefore define Σcycl as [(**20**) + (**21**)]. The unidentified 〰Phen isomer (**25**) is much less important, and, in the absence of further information on its structure, we have not included it in Σcycl.

The time evolution plot of Σcycl vs. time at 375 °C (slope = 0.0087 mol % min^{-1}; $r^2 = 0.997$; Figure 1) has a time intercept of 4.9 min, and a maximum again occurs in the selectivity vs.

conversion plot (Figure 2). Hence, cyclization is characterized by the *same* initial transient inhibition behavior as rearrangement. Values of L'_{cycl}, defined as $\Sigma cycl/\Sigma C_7$'s, were calculated exactly as described above for L'_{rearr} and are compiled in Table VIII as a function of temperature, conversion, and coverage. As with rearrangement, L'_{cycl} is not very sensitive to temperature over the small range studied but decreases markedly both with increasing conversion and decreasing coverage.

In contrast to the reaction pathways considered so far, there is no well-established mechanism for cyclization in the fluid state against which to compare the surface-attached behavior. We will explore possible mechanisms below. The important observation for the moment is that surface immobilization has promoted cyclization just as it did rearrangement. In addition, rearrangement and cyclization share the same brief initial inhibition period. And the quantities L'_{rearr} and L'_{cycl} respond similarly to reaction conditions (Table VIII). Hence, we suggest that cyclization also has chain character and thus is also enhanced by the restrictions on radical termination inherent in surface immobilization. In broad strokes, such a chain might be:

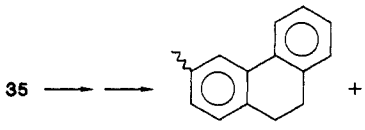

(10a)

H· + 16c → 35 + ? (11a)

Unsymmetrical Cleavage. In an ideal unsymmetrical cleavage of **16c**, the ratios ~~PhC$_2$H$_5$ (**22**):PhH (**10**) and (PhC$_2$H$_5$ (**11**) + PhC$_2$H$_3$ (**17**)):~~PhH (**23**) should each be 1.00. As shown in Table VI and Figure 2, each ratio appears to be slightly greater than unity, but the scatter associated with measuring these relatively minor products is large. The average value of the ratio [(**22**) + (**10**)]/[(**11**) + (**17**) + (**23**)] of 0.9 ± 0.1 (Table VI) reveals no selectivity between the two regiochemically distinct modes of cleavage. We define Σ(unsym cleav/2) as the sum of these five C_6 and C_8 products, divided by 2 to account for two molecules being formed in each cleavage event.

The linearized time evolution plot of Σ(unsym cleav/2) at 375 °C (Figure 1) shows an even larger intercept (7.7 min) than that for either Σrearr or Σcycl (4.6 and 4.9 min). A suspicion that this plot should in fact, have the same intercept but be curved upward slightly is raised by the slightly positive slopes in the selectivity-vs.-conversion plots for C_6 and C_8 products (Figure 2). The emergence of *both* unsymmetrical cleavage and cyclization as significant processes for **16c** compared with **1**, as well as the fact that unsymmetrical cleavage represents net hydrogen gain while cyclization represents net hydrogen loss, suggests searching for a mechanistic connection between them.

We being by examining the stoichiometric relationships between these processes. Consider a *carbon* stoichiometry where each molecule of ~~PhenH$_2$ (**20**) formed from **16c** is accompanied by l events of unsymmetrical cleavage:

$$(1 + l)\mathbf{16c} \rightarrow \mathbf{20} + l(\Sigma\text{unsym cleav}/2)$$

Consider also that each subsequent act of aromatization of **20** to form ~~Phen (**21**) is accompanied by l' additional events of unsymmetrical cleavage of **16c**:

$$\mathbf{20} + l'\mathbf{16c} \rightarrow \mathbf{21} + l'(\Sigma\text{unsym cleav}/2)$$

Then, at any point in the reaction, we have:

$$(\Sigma\text{unsym cleav}/2) = l(\mathbf{20}) + (l + l')(\mathbf{21})$$

which can be linearized in the form:

$$\frac{(\Sigma\text{unsym cleav}/2)}{(\mathbf{20})} = l + (l + l')\frac{(\mathbf{21})}{(\mathbf{20})}$$

where (**21**)/(**20**) is, in essence, a measure of conversion level. Omitting the three entries in Table III with probable outliers, we have seven points at high coverage to fit to this form. Least-squares analysis gives $l = 0.57$; $(l + l') = 0.98$ [i.e., $l' = 0.41$]; $r^2 = 0.98$. The nonzero value of l', indicative of the fact that the secondary conversion of **20** to **21** does induce some unsymmetrical cleavage, explains the slightly positive slopes for C_6 and C_8 products in Figure 2 and the suspected (see above) upward curvature for Σ(unsym cleav/2) in Figure 1.

Within experimental uncertainties, l and l' are most likely equal; i.e., the same mode of unsymmetrical cleavage is likely induced by both the formation and consumption of **20**. Remembering the characteristic ability of hydrogen atom to effect such cleavage of **1**,[33,34] we suggest that surface-immobilized steps 8a and 9a are responsible. However, since $l \simeq l' < 1.0$, we suggest also that hydrogen atom transfer step 8b is about as rapid as aromatic substitution step 8a. In fact, the amount of H_2 produced in the run where it was measured is fully consistent with l and l' values near 0.5. As an analogy, note that hydrodealkylation (as in step 8a) and benzylic hydrogen abstraction (as in step 8b) are actively competitive during interaction of hydrogen atom with toluene.[47] In this formulation, step 11a is the sum of step 8b and the sequence 8a plus 9a, each of which transforms hydrogen atom and **16c** to radical **35**.

H· + **16c** → ~~PhH (or PhH) + PhCH$_2$CH$_2$· (or ~~PhCH$_2$CH$_2$·) (8a)

PhCH$_2$CH$_2$· (or ~~PhCH$_2$CH$_2$·) + **16c** → PhCH$_2$CH$_3$ (or ~~PhCH$_2$CH$_3$) + **35** (9a)

H· + **16c** → **35** + H$_2$ (8b)

Possible Mechanisms for Cyclization. Just as surface immobilization enhanced rearrangement without a fundamental change in elementary steps from that in the liquid state, so we assume that it has enhanced cyclization. In fact, by use of more sensitive analytical techniques than used in our previous liquid-phase studies,[12] we have observed[31] traces of 9,10-dihydrophenanthrene as well as phenanthrene at lower conversions. How then might step 10, and, by analogy, step 10a occur? A thermochemical kinetic analysis of reaction channels available to radical 4 in the liquid state is useful in testing hypothetical mechanisms. We estimate the relative rates of production of the series of products Z arising from 4 (Table I) for which:

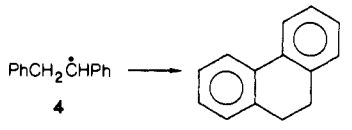

(10)

$$d(Z)/dt = k_Z(4)$$

where k_Z is the appropriate first-order rate constant or product of a second-order rate constant and a reagent concentration. Taking the necessary rate constant estimates from Miller and Stein's detailed modeling study,[13] we estimate k_Z at 375 °C and 1 M **1** (as a concentration standard state) and the corresponding $\Delta G^{\ddagger}_{648}$, the highest point on the free-energy profile starting from

Table IX. Estimated Rate Constants and Free Energies of Activation for Reaction Channels Available to PhCH$_2$ĊHPh (**4**)

reaction (step(s))	rate expression	k_Z (s^{-1})[a]	k_Z^{648} (s^{-1})[b,c]	$\Delta G^{\ddagger}_{648,Z}$ (kcal mol^{-1})[d]
hydrogen transfer (12)	k_{12} (**1**) (**4**)	k_{12} (**1**)	1600[e]	29
coupling (4)	k_4 (**4**)^2	$(k_1k_4)^{1/2}$ (**1**)$^{1/2}$[f]	55[g]	34
rearrangement (5, −5, 6)	K_5k_6 (**1**) (**4**)	K_5k_6 (**1**)	12[h]	36

[a] Rate = d(Z)/dt = k_Z (**4**). [b] Rate constant estimates from ref 13. [c] (**1**) assigned as 1 M. [d] $\Delta G^{\ddagger} = -RT \ln (k_Zh/k_BT)$. [e] k_{12} taken as estimate for similar reaction between **4** and **7**; $10^{8.62}$ exp(−16 060/RT) M^{-1} s^{-1}. [f] $(\mathbf{4})_{ss} = (k_1/k_4)^{1/2}(\mathbf{1})^{1/2}$. [g] $k_1 \simeq 10^{15.9}$ exp(−65 000/RT) s^{-1}; $k_4 \simeq 10^{9.5}$ M^{-1} s^{-1}. [h] $k_5 \simeq 10^{13}$ exp(−23 500/RT) s^{-1}; $k_{-5} \simeq 10^{13}$ exp(−9000/RT) s^{-1}; $k_6 \simeq 10^{8.62}$ exp(−7900/RT) M^{-1} s^{-1}.

(47) Price, S. J. *Can. J. Chem.* **1962**, *40*, 1310.

radical 4. These estimates are compiled in Table IX.

The most rapid process is hydrogen atom transfer step 12 with $\Delta G^{\ddagger}_{648} \simeq 29$ kcal mol^{-1}. Although normally "invisible", its facile

$$4 + \mathbf{1} \rightarrow \mathbf{1} + 4 \qquad (12)$$

occurrence is supported by Benjamin's isotopic exchange studies[48] of the thermolysis of $PhCD_2CD_2Ph$ (**1**-d_4) in tetralin. Note for possible future investigation that an analogous process in the surface-attached state (step 12a) would provide a pathway for

$$\underset{\mathbf{35}}{\sim\!\sim PhCH_2\dot{C}HPh} + \underset{\mathbf{16c}}{\sim\!\sim PhCH_2CH_2Ph} \rightarrow \mathbf{16c} + \mathbf{35} \qquad (12a)$$

slow "migration" of the radical center in **35** over the surface by chemical reaction rather than physical diffusion. The major observed reaction of 4 in the liquid state is self-coupling, step 4, with $\Delta G^{\ddagger}_{648} \simeq 34$ kcal mol^{-1}.[49] The second observed reaction is rearrangement by steps 5 and 6, with $\Delta G^{\ddagger}_{648} \simeq 36$ kcal mol^{-1}. If cyclization in the liquid state is about one order of magnitude less facile than rearrangement (Table I), then the estimates summarized in Table IX suggest that its $\Delta G^{\ddagger}_{648}$ must be ~39 kcal mol^{-1} [$\exp(\Delta\Delta G^{\ddagger}/648R) = 10$ for $\Delta\Delta G^{\ddagger}_{648} = 3$ kcal mol^{-1}].

Miller and Stein[13] suggested a cyclization pathway wherein addition of the ortho carbon of the delocalized benzylic radical 4 to the second phenyl ring generated radical **37**. However, because of the very unfavorable estimated enthalpy of step 13,

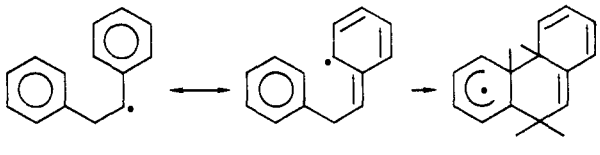

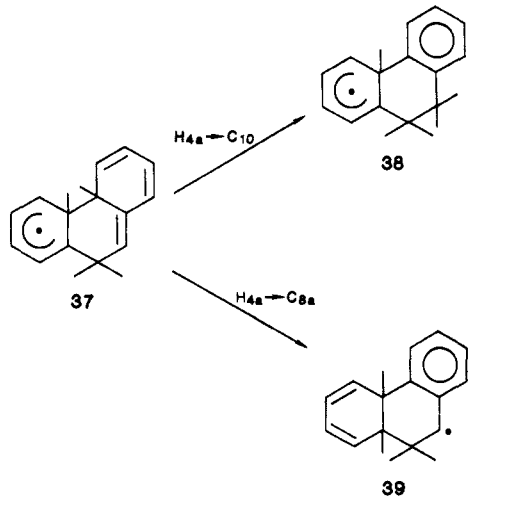

they suggested that it was somehow concerted with one of two 1,3-hydrogen shifts to restore aromaticity (step 14 or 14'). Noting, however, that the 1,3-sigmatropic shift proposed in step 14 is orbital symmetry-forbidden and that the 1,3-shift proposed in step 14' somehow passes "through" a saturated carbon, we are unaware of precedents for such a concerted radical addition–hydrogen shift. We do not see, therefore, how this cyclization hypothesis can avoid paying the enthalpy cost of forming **37** as a true intermediate. We have made thermochemical kinetic estimates (see Appendix 2) for several conceivable decay routes for **37**. For expulsion of hydrogen atom to form 4a,9-dihydrophenanthrene (**40**), $\Delta G^{\ddagger}_{648}$ appears to consist of $(\Delta G^{\circ}_{13} + \Delta G^{\circ}_{15} + \Delta G^{\ddagger}_{-15})_{648}$ and to lie some (31 + 12 + 14) ≃ 57 kcal mol^{-1} above 4. The very large difference between this estimate and our "target" of 39 kcal mol^{-1} calls this pathway into serious question. This hydrogen expulsion barrier might be lowered if step 15 were coupled with step 8.

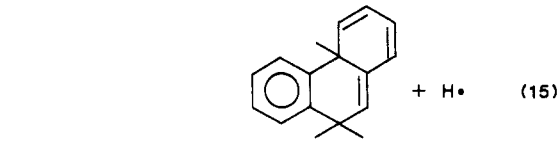

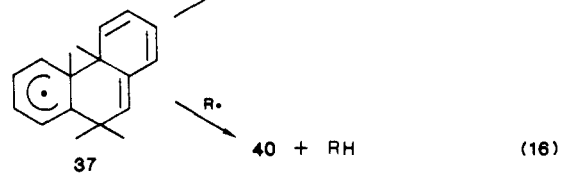

However, the considerations outlined by McMillen and coworkers[50] show the present case to be particularly unfavorable for this concerted alternative because of the minimal polycyclic aromatic stabilization in **37**. A second decay route might be conversion to **40** by disproportionation with a second radical (step 16). However, we estimate this to be even less favorable than step 15. A third decay route might be 1,3-hydrogen migration step 14 as a discrete step.[51] However, we estimate its barrier $(\Delta G^{\circ}_{13} + \Delta G^{\ddagger}_{14})_{648}$ as $\gtrsim 58$ kcal mol^{-1}. In summary, we see no obvious kinetically competent cyclization pathway passing through radical **37**.

We therefore present for examination an alternate cyclization hypothesis which begins with an intramolecular 1,4-hydrogen atom transfer to form aryl radical **41** (step 17) followed by intramo-

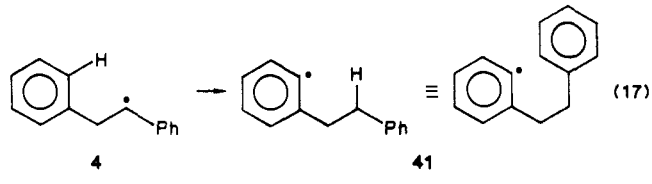

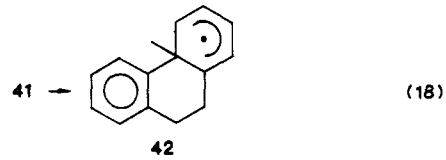

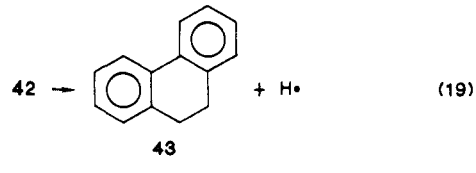

lecular addition to form **42** (step 18) followed by hydrogen atom expulsion (step 19) to form 9,10-dihydrophenanthrene (**43**). We estimate that the highest point on the free-energy profile for this sequence of steps lies at the initial step 17 and that $\Delta G^{\ddagger}_{648,17} \simeq 41$ kcal mol^{-1} (Appendix 2). Because this value is so much closer to our "target" of 39 kcal mol^{-1}, we conclude that a cyclization route via steps 17, 18, and 19 appears thermochemically more feasible than any route beginning with step 13. Although such approximate analysis does not, of course, demonstrate a mechanism, future studies should include this route among viable cyclization hypotheses.

Implications for Coal Conversion. The essential invariance of the rate of homolysis of the $PhCH_2$–CH_2Ph bond in surface-immobilized **16c** compared with that of **1** in the liquid or gas phase gives added confidence to the extrapolation of bond homolysis rates from $ArCH_2CH_2Ar'$ model compounds to dimethylene bridges ($-ArCH_2CH_2Ar'-$) in coal. On the other hand, the greater extents of skeletal rearrangement, cyclization, and unsymmetrical cleavage

(48) Benjamin, B. M.; Michalczyk, M. J.; Woody, M. C. *Proc. AIChE Mett.* June, 1980.

(49) Note that radical coupling is still being considered as an unactivated process ($E \simeq 0$). The large positive $\Delta G^{\ddagger}$ results from the formalism of including the very low value of $(\mathbf{4})_{\text{steady-state}} \sim 1.7 \times 10^{-8}$ M in the "first-order" rate constant k_{coupling}.

(50) McMillen, D. F.; Malhotra, R.; Chang, S.-J.; Nigenda, S. E. *Prepr. Div. Fuel Chem., Am. Chem. Soc.* **1985**, *30* (4), 334.

(51) It is difficult to rigorously rule out an acid- or base-catalyzed conversion of **37** to **38**.

observed with **16c** compared with **1** suggest that greater concern needs to be given to analogous processes in coal than would have been indicated by results from **1** alone. If the technological goal is liquefaction or pyrolysis to form depolymerized products, the observed skeletal rearrangement of $-ArCH_2CH_2Ar'-$ units to

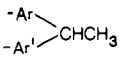

units is undesirable in that a thermally sensitive cross-link is converted to a more stable one. Cyclization of $-ArCH_2CH_2Ar'-$ units to phenanthrene units is even less desirable on this basis (but may be desirable for coking). Each of these undesirable pathways is a chain process originating from $-ArCHCH_2Ar'-$ radicals formed by hydrogen atom abstraction from the coal backbone. Thus, good hydrogen atom donor solvents, DH, should play a crucial role in liquefaction not only by capturing $-ArCH_2\cdot$ radicals, but also by transferring the radical centers in $-ArCHCH_2Ar'-$ to solvent-derived radicals, D·. Since such D· radicals are much more free to diffuse and hence terminate chains than are the $-ArCHCH_2Ar'-$ radicals which are still attached to the coal framework, the net result should be chain inhibition as desired. To fulfill this anticipated chain inhibiting role, however, the donor solvent must have permeated throughout the coal matrix and be present at the exact locale where $-ArCHCH_2Ar'-$ radicals are formed.

Experimental Section

GC analyses were performed on a Hewlett-Packard 5880A gas chromatograph equipped with a 12 m × 0.25 mm i.d. wall-coated OV-101 capillary column and a flame ionization detector. A typical temperature program consisted of a 1-min hold at 40 °C, a 10 °C min^{-1} ramp to 270 °C, and a 10-min hold at 270 °C; these conditions were sufficient to elute materials of as low a volatility as trimethylsilylated C_{28} diphenols. Areas from electronic integration of the flame ionization detector signal were converted to molar units by calibration factors with respect to internal standards; these were determined experimentally in all cases where authentic samples were available (see below) and otherwise estimated from carbon numbers. Mass spectra (70 eV) were determined with a Hewlett-Packard 5995A gas chromatograph–mass spectrometer equipped with a bonded-phase methylsilicone capillary column. NMR spectra were determined with a Nicolet NT-200 spectrometer and chemical shifts are expressed relative to Me_4Si. DRIFT spectra were obtained on a Digilab FTS-20c spectrometer by co-adding 100 scans measured at 4-cm^{-1} resolution on specimens prepared by mixing 30 mg of sample with 300 mg of dry KBr in a Wig-L-Bug mixer. Spectra were plotted in the Kubelka-Munk format which is reported to give spectra that are in close approximation to the corresponding absorbance spectra for samples prepared as KBr disks.[52]

Phenols 15a–d. Commercially available *p*-phenylphenol (**15a**) was recrystallized from ethanol–water, and *p*-benzylphenol (**15b**) was sublimed. Each was 99% pure by GC analysis. *p*-(2-Phenylethyl)phenol (**15c**) was prepared by hydrogenation of commercially available *trans*-*p*-hydroxystilbene (5 g) in ethanol solution (100 mL) over 10% Pd/carbon catalyst (0.75 g) for 2 days at room temperature and 40 psig (375 kPa) hydrogen pressure. Crystallization from ethanol–water, elution from an alumina column with petroleum ether–ethanol (1:1), and recrystallization gave **15c** which was 99.99% pure by GC analysis. *p*-(3-Phenylpropyl)phenol (**15d**), 96% pure by GC analysis, was prepared by catalytic hydrogenation of *p*-cinnamylphenol which was obtained by alkylation of phenol with cinnamyl alcohol in aqueous citric acid–ascorbic acid as described by Jurd.[53]

Surface-Attached α,ω-Diphenylalkanes 16a–d. A preparation of $\sim PhCH_2CH_2Ph$ (**16c**) is described as typical. Fumed silica (Cabosil M-5, Cabot Corp., 200 ± 25 $m^2\ g^{-1}$) was dried for several hours at 210 °C in air. A slurry of 8 g of silica [(8 g)(2 × 10^{20} $nm^2\ g^{-1}$)(~5 OH nm^{-2})(1 mmol/6 × 10^{20} OH) ≃ 13 mmol surface OH groups] in benzene, freshly distilled from lithium aluminum hydride, was mixed with a solution of 4.8 g (24.2 mmol) of phenol **15c** in benzene. Benzene was gradually removed on a rotary evaporator to a final temperature and pressure of 80 °C and 3 Pa. The resulting solid was transferred to a Pyrex tube and thoroughly degassed by repetitive evacuation and purging with argon. [Note: Evacuation must be done with care because of the fluffy character of the silica.] The tube was finally evacuated to 0.5 Pa, sealed, and heated fully within the confines of a tube furnace for 1 h at 220 °C. It was then cooled, opened, connected to a vacuum of 0.7 Pa, and heated for 0.5 h at 300 °C to remove excess **15c**. The final white, free-flowing powder (bulk density = 0.1 – 0.15 g mL^{-1}) was homogenized well in a Mini-mill before use. Assay as described below indicated 0.465 mmol of $\sim PhCH_2CH_2Ph$ per g of final product. Material with lower coverages was prepared by limiting the amount of **15c** used.

Assay Procedure. An assay of **16c** is described as typical. A weighed sample of **16c** (~0.1 g) was stirred overnight at room temperature with 10 mL of 1 N sodium hydroxide solution. To the resulting clear solution was added a measured aliquot (~1 mL) of a solution of an internal standard for GC analysis, typically phenol **15a** dissolved in 1 N sodium hydroxide. The mixture was acidified and extracted thoroughly with methylene chloride. The extracts were dried over anhydrous sodium sulfate and the solvent was evaporated. The residual phenols were heated for 15 min on a steam bath in 0.2 mL of a 3:1 (v:v) mixture of bis(trimethylsilyl)trifluoroacetamide (BSTFA) and pyridine, and the resulting trimethylsilyl derivatives were analyzed by GC.

Thermolysis Procedure. The desired amount of surface-attached material (0.25–0.5 g) was loaded into one arm of a T-shaped Pyrex tube (8 mm i.d.) which was then evacuated and sealed. A horizontal temperature-controlled tube furnace was fitted with an internal copper cylinder containing a central cylindrical hole just large enough to accommodate the tube and an externally attached thermocouple. The sample-containing arm was inserted into the preheated furnace (±1 °C) while the vertical leg was simultaneously placed in a liquid nitrogen bath. After the desired heating period, the tube was removed from the furnace, quickly cooled, and opened. Volatile products condensed in the cold trap were collected in a minimal volume of acetone and analyzed by GC with *p*-xylene and 2,2-diphenylpropane as internal standards. After evaporation of the acetone, phenol **15c** in the cold trap was trimethylsilylated and analyzed by GC as described above with phenol **15a** as an internal standard. The solid residue in the heated arm was assayed for phenols by digestion in aqueous base, trimethylsilylation, and GC analysis as described above with 2,5-dimethylphenol and **15a** as internal standards. In selected cases, the solid residue was digested instead in 1 N hydrochloric acid. Although this did not produce complete dissolution of the silica, extraction and trimethylsilylation gave GC patterns fully analogous with those from digestion in base. This observation precludes the possibility that acid or base catalysis during the workup procedure altered the thermally produced surface-attached products.

Product Assignments. Provisional product assignments were based on retention times and were confirmed by comparison of mass spectra with those of authentic materials, generally after trimethylsilylation for the phenolic products. Samples of the nonphenolic products **1**, **3**, **6**, **10**, **11**, and **17** were all commercially available. The phenols corresponding to surface-attached products **19**, **22**, **23**, **24**, and **27** were also commercially available.

p-(1-Phenylethyl)phenol, corresponding to **18**, was prepared by acid-catalyzed alkylation of phenol with styrene[54a] and purified[54b] by vacuum distillation: parent and base *m/z* 198 and 183 ($HOC_6H_4CHC_6H_5^+$); after trimethylsilylation 270 and 255.

An authentic archival sample of 3-phenanthrenol, corresponding to **21**, was kindly supplied by B. M. Benjamin.[55] Additional material was prepared as follows. *trans*-*p*-Hydroxystilbene (13.5 g, 69 mmol) was methylated with methyl iodide (30 g, 211 mmol) in a refluxing mixture of tetrahydrofuran (300 mL) and aqueous tetrabutylammonium hydroxide (70 mL, 105 mmol) by the method described by Liotta.[56] A solution of this *trans*-*p*-methoxystilbene (0.5 g) in 1,2-dimethoxyethane (50 mL) containing iodine (0.03 g) and exposed to air was photolyzed in a quartz tube with a 400-W mercury lamp for several hours by the procedure of Malllory and Wood.[57] 3-Methoxyphenanthrene was produced in 50–60% yield (GC) and was purified (92%) by elution from an alumina column with petroleum ether. Demethylation by pyridine hydrochloride by the method of Anderson et al.[43] (details for an analogous example below) gave 3-phenanthrenol: *m/z* (rel intensity) after trimethylsilylation 266 (100), 251 (80), and 125.5 (41).

9,10-Dihydro-3-phenanthrenol,[58] corresponding to **20**, was prepared as follows. 3-Methoxyphenanthrene (250 mg) was hydrogenated in ethyl acetate solution (8 mL) over 10% Pd/carbon catalyst (70 mg) for 3 days

(52) Wang, S.-H.; Griffiths, P. R. *Fuel* **1985**, *64*, 229. Fuller, M. P.; Griffiths, P. R. *Anal. Chem.* **1978**, *50*, 1906.
(53) Jurd, L. *Tetrahedron Lett.* **1969**, 2863. Jurd, L.; Stevens, K. L.; King, A. D.; Mihara, K. *J. Pharm. Sci.* **1971**, *60*, 1753.
(54) (a) Koenigs, W.; Carl, R. W. *Ber.* **1891**, *24*, 3889. (b) Pickard, R. H.; Littlebury, W. O. *J. Chem. Soc.* **1906**, *89*, 467.
(55) Collins, C. J.; Benjamin, B. M. *J. Am. Chem. Soc.* **1953**, *75*, 1644.
(56) Liotta, R.; Brons, G. *J. Am. Chem. Soc.* **1981**, *103*, 1735.
(57) Mallory, F. B.; Wood, C. S. *Organic Synthes* Collect. Vol. V.; Wiley: New York, 1973; p 952.
(58) Takaki, K.; Okada, M.; Yamada, M.; Negoro, K. *J. Org. Chem.* **1982**, *47*, 1200.

at room temperature and 20 psig (240 kPa) hydrogen pressure followed by an additional 4 days with fresh catalyst.[59] Chromatography on alumina gave 3-methoxy-9,10-dihydrophenanthrene as an oil of 90% purity (the dominant impurity was *p*-methoxybibenzyl formed by hydrogenation of the *p*-methoxystilbene impurity in the starting material): ^{1}H NMR ($CDCl_3$) δ 2.80 (br s, 4 H), 3.82 (s, 3 H), 6.8 (m, 1 H), 7.10–7.28 (m, 5 H), and 7.70 ppm (d, 1 H, J = 7 Hz); UV (CH_3OH) λ_{max} 263 (ϵ ~15000) and 305 nm (ϵ ~6600) (lit.[60] for 9,10-dihydrophenanthrene (EtOH) λ_{max} 264 (ϵ 17,000) and 300 nm (ϵ 4500)); *m/z* (rel intensity) 210 (100), 209 (44), 179 (32), and 165 (44). Demethylation by pyridine hydrochloride[43] gave 9,10-dihydro-3-phenanthrenol: *m/z* (rel intensity) after trimethylsilylation 268 (100) and 253 (62).

The trimethylsilylated phenol, corresponding to **25**, had a GC retention time slightly longer than that of trimethylsilylated 3-phenanthrenol but a very similar mass spectrum. It has not been conclusively identified.

The trimethylsilylated phenols, corresponding to **26**, consisted of two GC-resolvable peaks in similar amounts both having a parent *m/z* 360 ($Me_3SiOC_6H_4C_3H_5Ph_2$). The first, having dominant *m/z* (rel intensity) 269 (100) and 91 (38), is tentatively assigned as $Me_3SiOC_6H_4CH(CH_2Ph)_2$. The second, having dominant *m/z* (rel intensity) 179 (100) and 180 (19), is tentatively assigned as $Me_3SiOC_6H_4CH_2CH(Ph)CH_2Ph$.

The trimethylsilylated phenol, corresponding to **28**, had a parent *m/z* of 268 but a GC retention time different from either that of trimethylsilylated *trans-p*-hydroxystilbene or its cis isomer, prepared by short photoisomerization of the trans. If small amounts of surface-attached *cis*-stilbene are formed (quite probably in equilibrium with the trans), they would be obscured in the GC analyses by residual trimethylsilylated **15c**.

Dehydrodimers of 15c. *p*-Methoxybibenzyl (**30**), mp 59.5–60.5 °C, was prepared from phenol **15c** by the Liotta methylation procedure.[56] A mixture of 8 g (38 mmol) of **30** and 1.9 g (13 mmol) of di-*t*-butyl peroxide was heated at 140 °C under N_2 for 24 h.[43] Chromatography on alumina allowed removal of unconverted **30** by elution with petroleum ether and recovery of the crude oxidatively coupled product (2.0 g) with acetone–petroleum ether (1:4). GC analysis revealed five partially resolved, closely spaced peaks in an area ratio of ~16:20:46:8:11; all had a parent *m/z* 422. Concentrated hydrochloric acid (33 mL) was added slowly to pyridine (30 mL) with cooling. This mixture was then heated at 210 °C until distillation of water was complete. The crude coupling product (1.5 g) was added at ~150 °C and heating was continued under N_2 at 180 °C for 3 h. The cooled product was partitioned between water and methylene chloride. The combined methylene chloride extracts were extracted with aqueous alkali to recovery phenolic products. Acidification gave the crude mixed dimeric phenols (**32a–c**) as a fibrous white solid: ^{1}H NMR ($CDCl_3$) δ 2.5–3.4 (m, benzylic), 4.9 (br, phenolic), and 6.4–7.4 ppm (m, aromatic) in a ratio of 18.6:1.8:5.7 (expected 18:2:6). GC analysis, after trimethylsilylation, showed a pattern virtually identical with that before demethylation: five partially resolved peaks in an area ratio of ~17:19:46:8:10, all with a parent *m/z* 538. Mass spectra were simpler and more structurally distinctive at the methylated than trimethylsilylated state. With the assumption that the major charge-carrying fragments will combine the benzylic and *p*-methoxy stabilizing features, tentative structural assignments were made as follows. The first two peaks (in order of increasing retention time as listed above) had a base *m/z* 211 ($PhCH_2CHAn^+$) with $I_{211}/I_{121} > 10$; thus these appear to be diastereoisomers of $PhCH_2CHAnCHAnCH_2Ph$ (**31a**) (An ≡ *p*-$CH_3OC_6H_4$–). The last two peaks had a base *m/z* 121 ($AnCH_2^+$) with $I_{211}/I_{121} < 0.01$; thus these appear to be diastereoisomers of $AnCH_2CHPhCHPhCH_2An$ (**31b**). Finally, the major central peak had $I_{211}/I_{121} = 3$; thus it appears to be the unresolved diastereoisomers of the unsymmetrical $PhCH_2CHAnCHPhCH_2An$ (**31c**). These assignments suggest that **31a**, **31c**, and **31b** were formed in a ratio of ~1.9:2.5:1. If the radicals $AnĊHCH_2Ph$ and $AnCH_2ĊHPh$ were formed by hydrogen abstraction from **30** in a ratio of χ:1 and coupled indiscriminately to form dimers in the ratio χ^2:2χ:1, a value of χ = 1.3–1.4 would fit the structural assignments made and would also be reasonable for the expected selectivity of hydrogen abstraction by *tert*-butoxy radical at 140 °C.[61]

The dominant member of the mixture of long-retention-time trace impurities in **16c** (see text) also had a parent *m/z* 538 but a base *m/z* 447 (P – $PhCH_2$) which was not significant in any of the isomers of trimethylsilylated **32a–c**. Such high stability for a high *m/z* ion may indicate aryl–aryl coupling of **15c** mediated by oxygen, e.g., ($PhCH_2$–$CH_2C_6H_3(OH))_2$.

The trimethylsilylated diphenol, corresponding to **29**, had a GC retention time very similar to but apparently different from those of any of the trimethylsilylated isomers of **32a–c** or of the dominant initial trace impurity in **16c**.

Acknowledgment. An authentic sample of 3-phenanthrenol was kindly supplied by B. M. Benjamin. Preparations of **16a**, **16b**, and **16d** were performed by Janie E. Leach, SCUU Science Semester Participant from Centenary College, Shreveport, LA. DRIFT spectra were obtained by J. E. Caton, Jr.

Supplementary Material Available: Appendix 1 describing kinetic and thermodynamic considerations concerning fluid-phase thermolysis of bibenzyl; and Appendix 2 describing thermochemical kinetic considerations concerning possible cyclization routes for 1,2-diphenylethyl radical (8 pages). Ordering information is given on any current masthead page.

(59) Fu, P. P.; Lee, H. M.; Harvey, R. G. *J. Org. Chem.* **1980**, *45*, 2797.
(60) Beaven, G. H.; Hall, D. M.; Lesslie, M. S.; Turner, E. E. *J. Chem. Soc.* **1952**, 854.
(61) Poutsma, M. L. In *Free Radicals*; Kochi, J. K., Ed., Wiley: New York, 1973; Vol. II, Chapter 15.